FINAL REPORT ON CONTRACT NAS8-11158
PREPARED FOR
AEROSPACE ENVIRONMENT OFFICE
AERO-ASTRODYNAMICS LABORATORY
GEORGE C. MARSHALL SPACE FLIGHT CENTER
NATIONAL AERONAUTICS AND SPACE ADMINISTRATION
HUNTSVILLE, ALABAMA

THEORETICAL STUDY AND ENGINEERING DEVELOPMENT OF JIMSPHERE WIND SENSOR

BY

The G. T. Schjeldahl Company
Advanced Programs Division
Northfield, Minnesota

July 1965

Prepared by:
Clinton V. Eckstrom
Clinton V. Eckstrom
Project Engineer

Approved by:
William E. Palmquist
William E. Palmquist
Program Manager
E. A. Basquin
E. A. Basquin
Reports Editor

NOTE: Sections IV, V, and VI of this report were prepared by Dr. H. G. Heinrich, E. L. Haak, and R. J. Niccum, University of Minnesota.

FORWORD

This is the Final Report on Contract NAS8-11158 prepared by the Advanced Programs Division of the G. T. Schjeldahl Company, Northfield, Minnesota for the NASA George C. Marshall Space Flight Center, Huntsville Alabama. Mr. James R. Scoggins, Deputy Chief of the Aerospace Environment Office, Aero-Astrodynamics Laboratory at NASA/MSFC was the contract monitor. At the Schjeldahl Company, Clinton V. Eckstrom was Project Engineer; Ronald Albrecht, Les Hamann and Gaylord Gilbertson contributed. The measurements of drag coefficients and apparent mass were conducted under subcontract at the University of Minnesota by staff members of the Department of Aeronautics and Engineering Mechanics and a group of students of Aerospace Engineering with Messrs. Thomas C. Neitz and Robert A. Noreen being particularly instrumental.

This contract advanced the Jimsphere concept from prototype models to production units now being used regularly for investigation of wind conditions prior to missile launches, space vehicle design, and general meteorological studies. In addition, a better understanding concerning the dynamics of balloon motion was attained, resulting in new equations of motion for the Jimsphere and new equations for the determination of wind sensing error. The Jimsphere was proved to be an excellent wind sensor with flight capabilities believed to meet NASA requirements. This program started 27 February 1964 and was completed 1 June 1965.

ABSTRACT

16084

Jimsphere Wind Sensor balloons of 2-meter diameter having various sizes, shapes, and quantities of roughness elements (projections) molded into the balloon material, have been fabricated and flight tested to determine the optimum design for control of flow separation and stabilization of the sphere wake. The Jimsphere wind sensing balloon reaches an altitude of approximately 18 kilometers within one hour. Wind tunnel tests have been conducted to determine the drag coefficient of a model Jimsphere and full-scale tests were conducted to determine the apparent mass factor for the Jimsphere configuration. A considerable discrepancy exists between the drag coefficients determined from flight data and those determined in the wind tunnel. No explanation is given for this difference. Theoretical investigations of the Jimsphere have concerned development of the equations of motion which include effects of apparent mass and wind accelerations, determination of wind response capabilities and wind gradient error factors due to wind response lag.

Author

TABLE OF CONTENTS

TABLE OF CONTENTS

LIST OF FIGURES

LIST OF FIGURES

LIST OF FIGURES PAGE

LIST OF SYMBOLS

a_o	Acceleration of balloon prior to impact
a	Acceleration of balloon at impact of lost weight
B	Buoyancy of balloon = ρ Vol g
C_D	Drag coefficient
D	Aerodynamic drag
Dia	Balloon diameter
F_A	Magnitude of apparent mass force
ΣF	Sum of all external forces acting on balloon
g	Acceleration of gravity = 32.2 ft/sec^2
h	Altitude
K	Apparent mass factor = m'/B
L	Lag Distance
m_G	Mass of gas in balloon
m_s	Mass of balloon including accessories
m'	Apparent mass
n_o	a_o/g
n	a/g
R	Response length
R_e	Reynolds Number
S	Cross-sectional area of balloon
t	Time
W'	Weight of apparent mass = m'g
W_A	Weight of the accelerometer
W_G	Weight of gas within balloon

LIST OF SYMBOLS

W_L	Lost weight
W_n	Static weight of balloon system = $W_A + W_g + W_s + W_L - B$
W_R	Remaining weight = $W_A + W_g + W_s$
W_S	Weight of balloon skin
V_B	Velocity of Balloon
V_R	Relative velocity of the balloon with respect to the air
V_W	Velocity of the air
V_{X_B}	Horizontal balloon velocity
V_{X_W}	Horizontal wind velocity
V_{Z_B}	Vertical balloon velocity
VOL	Volume of balloon
$\dot{V}$	Acceleration
$\hat{v}$	Unit vector in the direction of the relative velocity
X	Horizontal position
Z	Vertical position
α	Velocity gradient
α_B	Balloon velocity gradient
α_W	Wind Gradient
μ	Mass ratio (displaced air mass to displacement mass)
ρ	Local air density
ξ_B	Wind gradient error factor

I. INTRODUCTION

A. General

The Jimsphere Wind Sensor is a 2-meter diameter spherical superpressure balloon with large roughness elements (projections) randomly located on the surface. The projections stabilize the airflow over the surface of the sphere and control flow separation on the sphere during operation at supercritical Reynolds number conditions. The Jimsphere Wind Sensor is used to measure small-scale wind motions in the atmosphere between ground level and approximately 18 kilometers altitude. Position of the Jimsphere during flight is determined by tracking with an AN/FPS-16 or similar radar, and balloon (wind) velocities are determined from the position data. Flight time from ground launch to maximum altitude for the Jimsphere is less than one hour.

B. Background

The Jimsphere balloon was conceived by James R. Scoggins of the NASA Marshall Space Flight Center to eliminate induced motions of previously used smooth-surfaced, 2-meter diameter, superpressure spheres which operated at supercritical Reynolds Numbers from ground level to approximately 11 kilometers altitude. Induced motions were not a problem at higher altitudes where the 2-meter diameter spheres operate at subcritical Reynolds Numbers conditions.

C. Engineering Developments and Theoretical Studies

Under this contract engineering developments of the Jimsphere balloon have been:

1. Fabrication of the roughness elements as integral parts of the Jimsphere balloon.
2. Determination of the size, shape and number of projections necessary to provide aerodynamic stability at supercritical Reynolds Number flow conditions.
3. Determination of the drag coefficient vs. Reynolds number curve of a Jimsphere model by wind tunnel test.
4. Determination of the apparent mass factors for the Jimsphere by full scale tests.

Theoretical investigations of the Jimsphere have included:

1. Development of the equations of motion including the effects of apparent mass and accelerating winds.
2. Derivation of the equation for wind response error.
3. Determination of the characteristic lag distances, response lengths, and distant constants.
4. Determination of the difference in Jimsphere velocity gradient and wind gradients (Wind Gradient Error Factors) for several conditions of altitude, Jimsphere rise-rate, and wind gradient conditions.

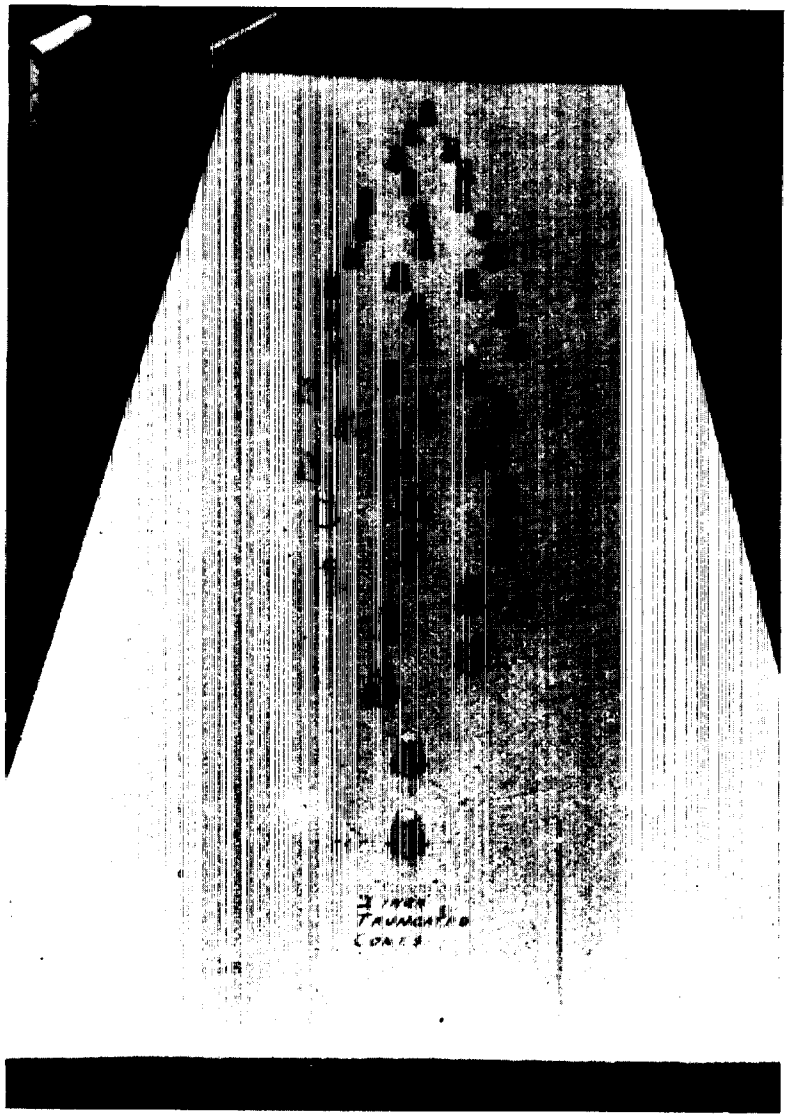

FIGURE 4. MOLD FOR FORMING GORES FOR JIMSPHERE MODEL 2-6-518T.

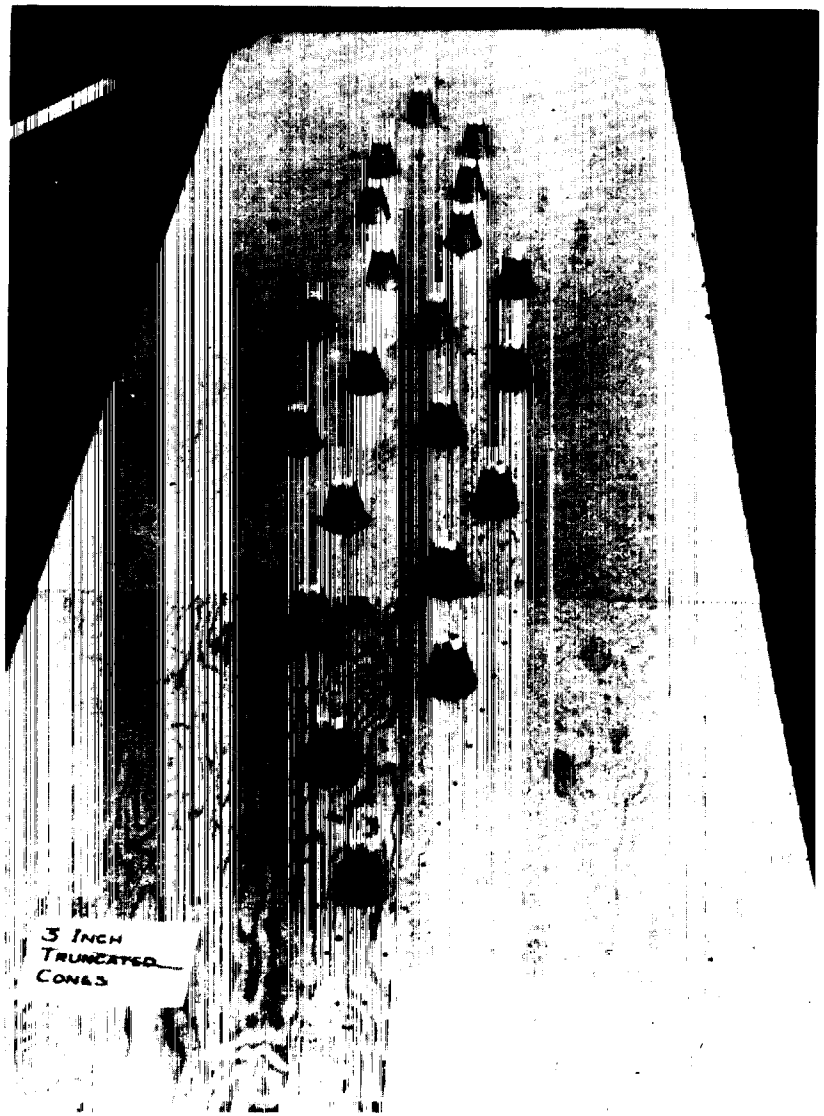

FIGURE 5. MOLD FOR FORMING GORES FOR JIMSPHERE MODEL 3-9-256T.

PROJECTION SPACING (INCHES)	TOTAL NUMBER OF PROJECTIONS FOR A 2-METER DIAMETER SPHERE
6	504
8	314
10	194

Mylar is drape formed in the following manner:

1. Stretch the Mylar film over the mold.
2. Heat the Mylar to near melting temperature. (Temperature control set at 580 F).
3. Create a vacuum in the area between the Mylar and the mold sucking the Mylar down onto the mold.
4. Allow the Mylar to cool on the mold.

Initially the capability existed to form half length gores only. A Jimsphere model 2-6-504T constructed using half gores is shown in Figure 3. Later the Schjeldahl Company drape former size was increased to allow forming of full length gores. The distribution of individual molds was then adjusted, resulting in an increase from 504 to 518 projections per sphere for the two-inch high projections on six inch spacings. The new gore mold is shown in Figure 4.

Jimspheres with three and four inch high projections were fabricated and flight tested to provide data on the effects of size and shape of roughness elements. Two different shapes of roughness elements were used on Jimsphere models having three-inch high projections. Jimsphere model 3-9-256T used roughness elements

an upper diameter of one and one-quarter inches, and a one-quarter inch radius on the upper edge of the cone. It was found that these projections could be formed in Mylar when placed as close together as six inches center to center.

C. Jimsphere Model Identification

To keep track of the various Jimsphere configurations fabricated, a model numbering system consisting of a series of numbers and a letter was used as shown.

MODEL 2-6-504T (example)

The first number indicates the projection height in inches, the second number indicates the nominal spacing distance in inches, and the third series of numbers indicates the total number of projections on the sphere. The letter following the numbers indicates the shape of the roughness element with T indicating a truncated cone and F indicating a full cone.

D. Gore Molds and Sphere Fabrication

Gore pattern molds for drape forming Mylar film were fabricated using the two-inch high projections with a shape as described in Paragraph B. To provide a variance in degree of roughness, three different spacings of the projections were used starting with the minimum possible spacing. The total number of projections per sphere for each projection spacing is listed below.

FIGURE 2. INFLATED MYLAR PILLOW WITH FORMED PROJECTIONS.

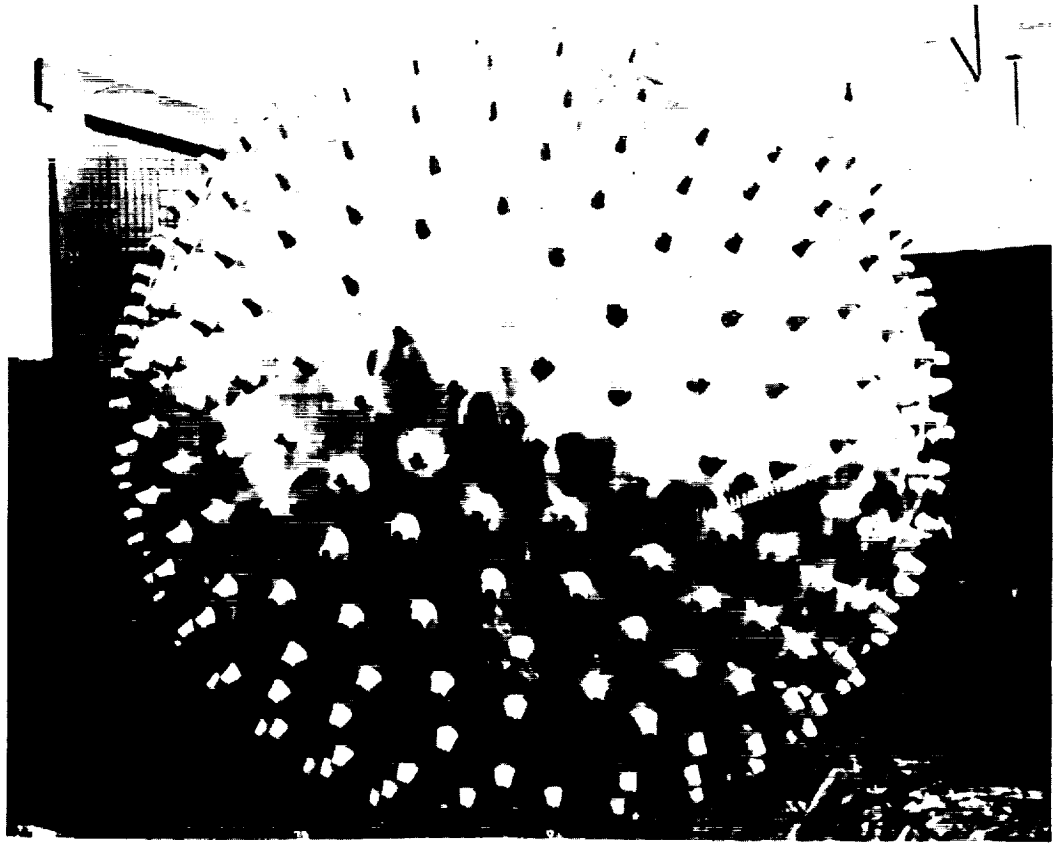

FIGURE 3. JIMSPHERE MODEL 2-6-504T CONSTRUCTED FROM FORMED HALF LENGTH GORES.

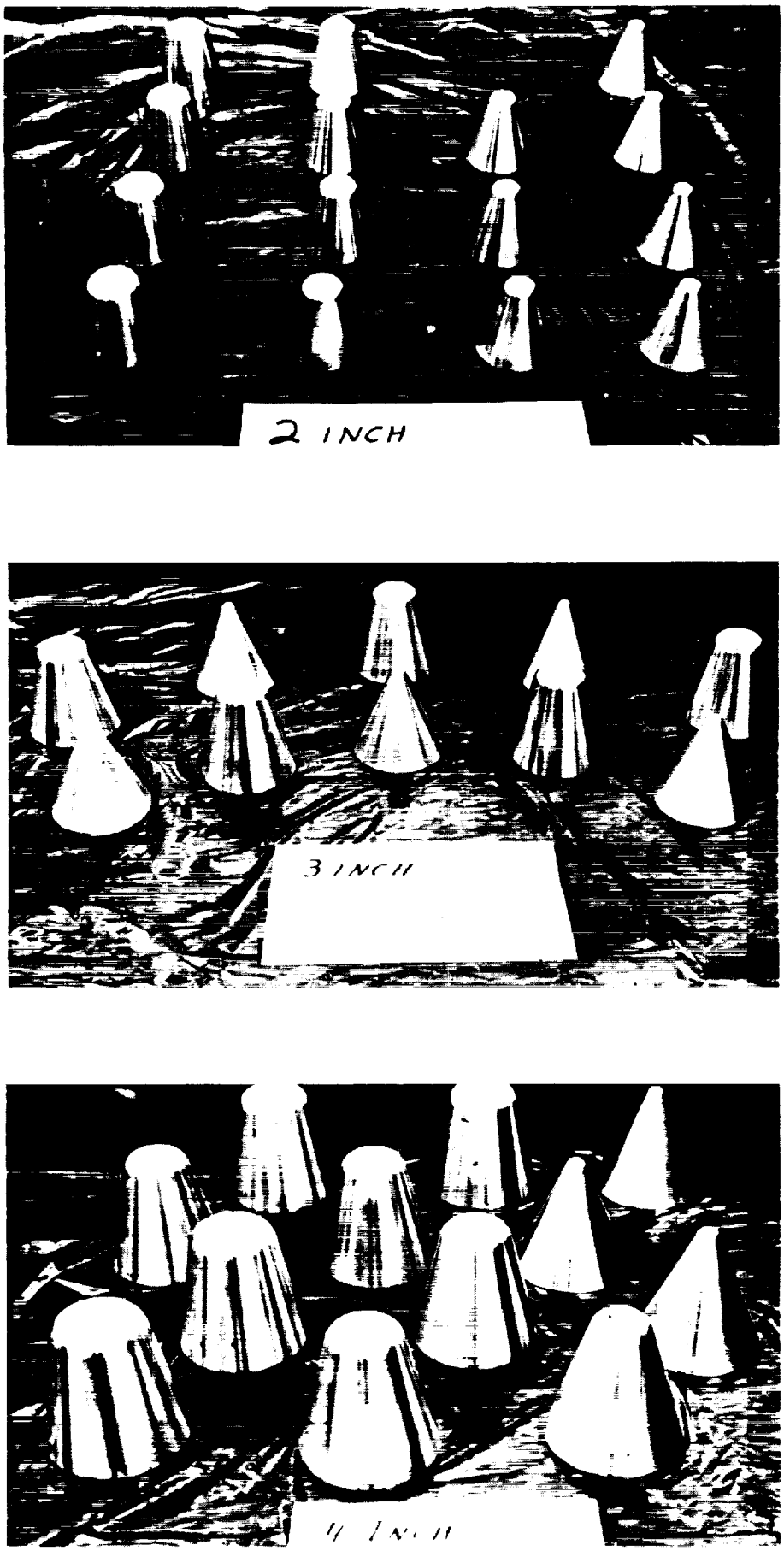

FIGURE 1. CONICAL ROUGHNESS ELEMENT MOLDS OF TWO, THREE AND FOUR INCH HEIGHTS.

II. DESIGN, FABRICATION AND TESTING OF VARIOUS JIMSPHERE CONFIGURATIONS

A. Design Guide

Investigations by Scoggins (Reference 1) in June of 1963 revealed that a 2-meter diameter superpressure sphere operating at supercritical Reynolds Number could be stabilized by adding roughness elements to the surface of the balloon. This new configuration was designated as a Jimsphere. Full-scale experimental flights conducted by Scoggins (Reference 2) at Cape Kennedy in August 1963, indicated that the roughness elements or protrusions should be 3 to 4 inches high and spaced approximately 6 to 8 inches apart. Using this information as a guide it was decided to investigate roughness elements of several types to establish the best Jimsphere configuration.

B. Roughness Element Design

Conical roughness element molds of various heights and proportions, as shown in Figure 1 were machined of aluminum. In all cases the base diameter of the roughness elements are the same as the height of the element. Mylar film was then drape formed over elements of each type, and small pillows, (shown in Figure 2) were fabricated to evaluate the inflated shape of the formed roughness elements. Shapes providing maximum cross-sectional area and sharp contours were sought.

Initially, roughness elements were formed in the shape of truncated cones two inches high with a base diameter of two inches,

which were a direct scale-up of the two-inch high truncated cones (3 inch height, 3 inch diameter base, upper diameter of 1 7/8 inches and a 3/8 inch radius on the upper edge). The gore mold for this design is shown in Figure 5.

Jimsphere model 3-7.5-398F used a full cone type projection having a height of 3 inches, a base diameter of 3 inches, and a 1/4 inch radius at the tip. The gore mold for this design is shown in Figure 6 and a fabricated sphere in Figure 7. One of the reasons for changing the projection shape from truncated cone to full cone was that full cones could be formed in the Mylar at much closer spacings, allowing many more projections per Jimsphere. Projection spacing was particularly critical on the Jimsphere having four-inch high projections, as the required spacing for truncated cones would have been 13 inches whereas the full cones were spaced at 8 inches. The Jimsphere Model 4-8-290F used a four-inch high projection which was a direct scale-up of the three-inch high full cone. The gore mold for the Jimsphere Model 4-8-290F is shown in Figure 8.

E. Flight Testing

Two spheres each of Models 2-10-194T, 2-8-314T, and 2-6-504T were fabricated and flight tested in April and May 1964 from Cape Kennedy, Florida. Visual observations of the flights indicated that balloon motions decreased as the degree of surface roughness increased. Radar track data as presented in Figure 9 confirmed

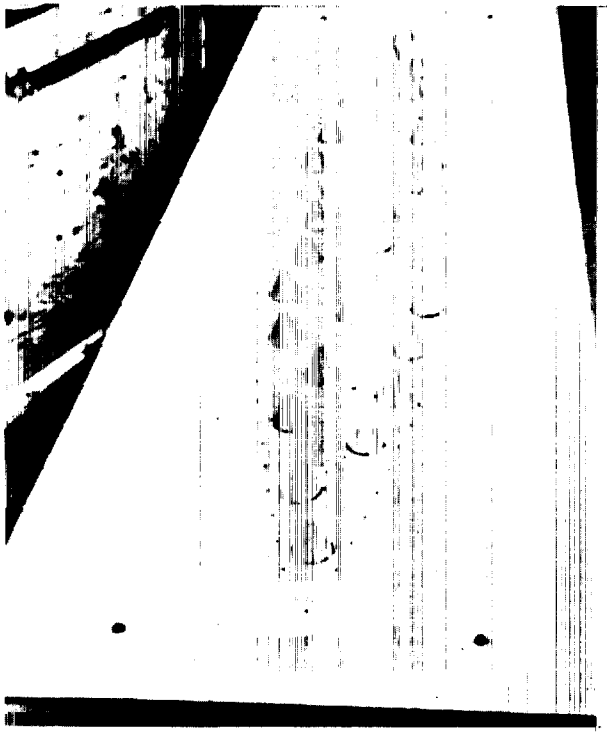

FIGURE 6. MOLD FOR FORMING GORES FOR JIMSPHERES MODEL 3-7.5-398F.

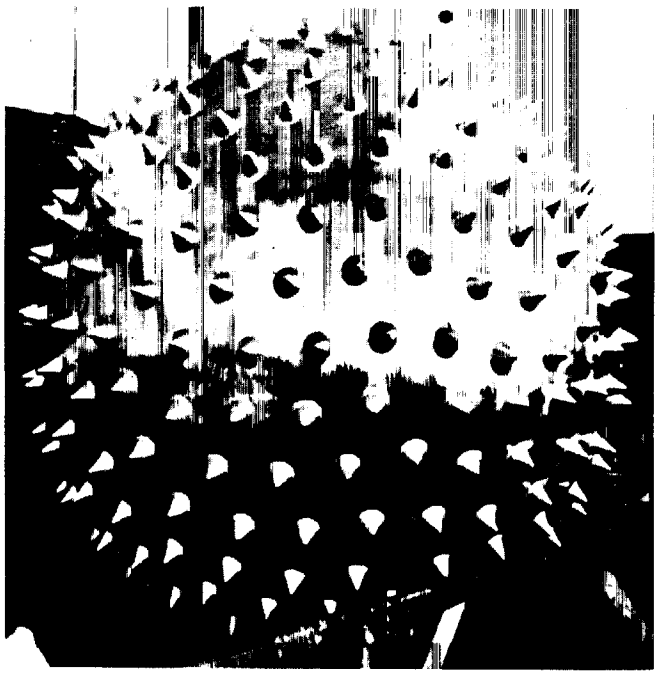

FIGURE 7. JIMSPHERE MODEL 3-7.5-398F.

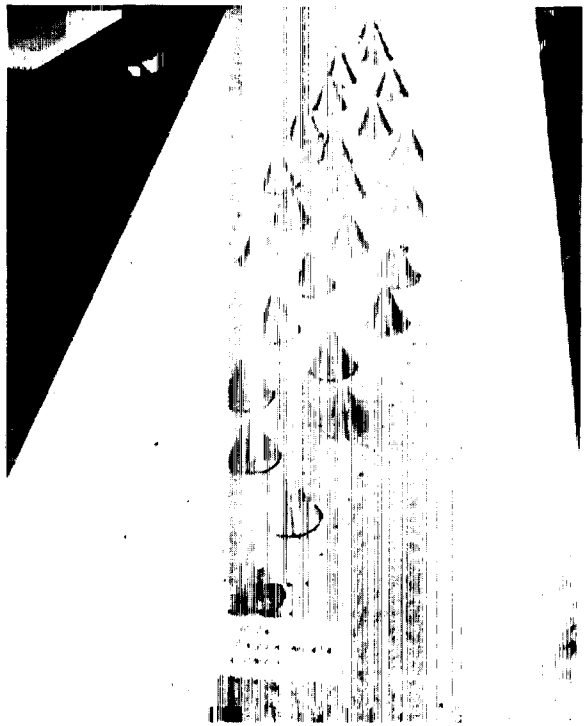

FIGURE 8. MOLD FOR FORMING GORES FOR JIMSPHERES MODEL 4-8-290F.

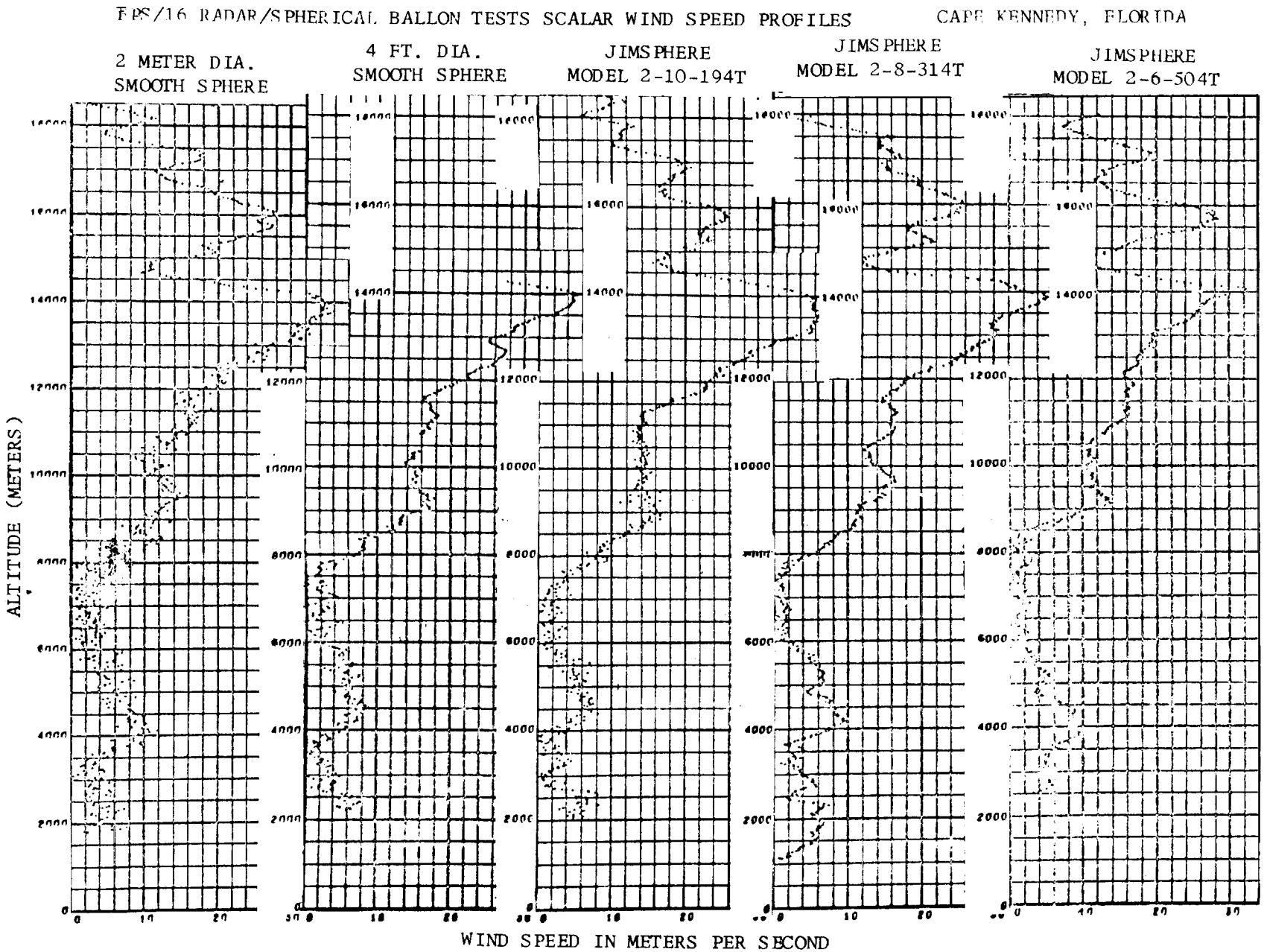

FIGURE 9 SCALAR WIND SPEED PROFILES FROM FLIGHT TESTS OF SEVERAL BALLOON CONFIGURATIONS

the visual observations.

Flight testing of Jimsphere Models 3-9-256T, 2-7.5-398F, and 4-8-290F was completed in June of 1964. An evaluation meeting was held in July and Jimsphere configurations 3-7.5-398F and 4-8-290F were selected for further study. A study of Jimsphere flight test movies by Marshall Space Flight Center personnel resulted in the observation that horizontal displacements of the balloon were associated with a rotation of the sphere. The observations indicated that the sphere rolled in the direction of horizontal movement. Further flight tests were proposed using 100 gram and 200 gram ballast weights attached to, or located in, the balloon hold down patch. Three Jimspheres each of Models 3-7.5-398F and 4-8-290F were fabricated and flight tested in August and September 1964 to determine the effects of ballast weights. In addition some modified Jimspheres were built and flown as reported in Appendix C.

III. SELECTED JIMSPHERE DESIGN

A. Detailed Description

The Jimsphere configuration shown in Figure 10 which is designated as Model 3-7.5-398F has been selected as the optimum design of those tested.

The Jimsphere wind sensing balloon Model 3-7.5-398F is a 2-meter diameter sphere with 398 conical roughness elements formed into 1/2 mil metalized Mylar used as the fabrication material. The sphere is constructed of 12 gores and two end caps. Six gores, spaced alternately, have 32 projections each and 34 projections are located in each of the remaining six gores. One projection is located in each of the end caps. The projections are full cones three (3) inches high, approximately three (3) inches in diameter at the base and spaced approximately 7.5 inches apart.

The Jimspheres have a lightweight plastic inflation valve, (See Figure 11), one-half inch in diameter and approximately one inch long. The inflation valve has a nylon diffuser bag and a snap-on closure cap. Two lightweight plastic pressure relief valves, spring loaded to provide 5 mb superpressure are located one each near the polar caps. A nylon load patch used to hold the balloon during inflation is located near the inflation valve. A 100 gram ballast weight used for stabilization purposes is located in the hold down patch. The average weight with ballast of 200 Jimspheres fabricated under Contract NAS8-13697 is 407.9 grams with standard deviation of 3.9 grams.

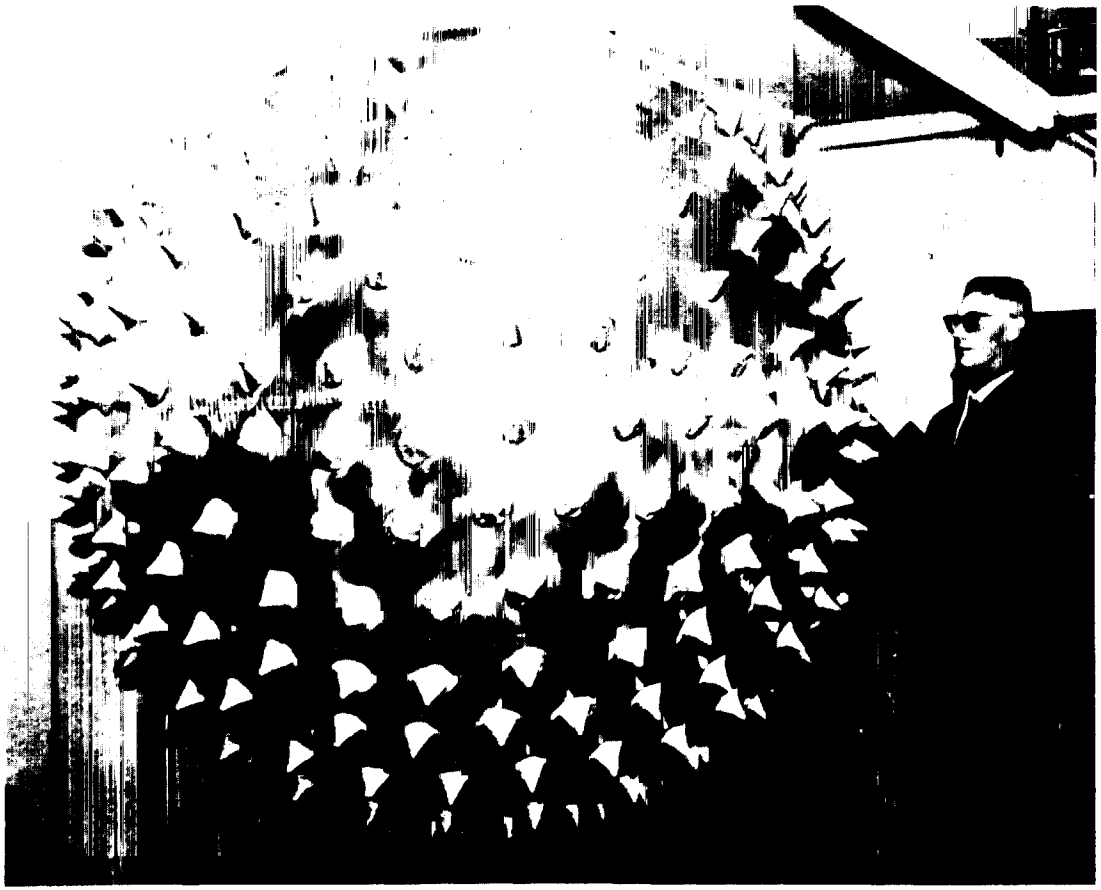

FIGURE 10. SELECTED JIMSPHERE DESIGN MODEL 3-7.5-398F.

FIGURE 11. END CAP VIEW OF JIMSPHERE MODEL 3-7.5-398F

A typical wind profile measurement made by tracking a Jimsphere Model 3-7.5-398F with the AN/FPS-16 radar and analyzing the data by the methods outlined in Reference 3 is presented in Figure 12.

B. Rise Rate Characteristics

Data from ten Jimsphere flights conducted in December 1964 have been evaluated to determine average rise rates as a function of altitude for the Jimsphere Model 3-7.5-398F. Rate of rise values were obtained from AN/FPS-16 radar track data which is presented in Appendix A.

The average rise rate for the ten flights is shown in Figure 13 along with the maximum and minimum average values from individual flights. All data which indicated a significant local deviation from normal were not used.

C. Coefficient of Drag from Flight Data

Drag coefficient values for the Jimsphere based on the above mentioned flight data are presented in Figure 14 as a function of Reynolds number. Calculations of the Drag Coefficients were based on:

1. The average values of rise rates from Figure 13.
2. A Jimsphere weight of 407.9 grams (average weight of 200 units produced on Contract NAS8-13697).
3. Atmospheric data for the month of December from Reference 4.
4. Values of balloon buoyancy based on use of helium inflation gas at 5 mb superpressure.

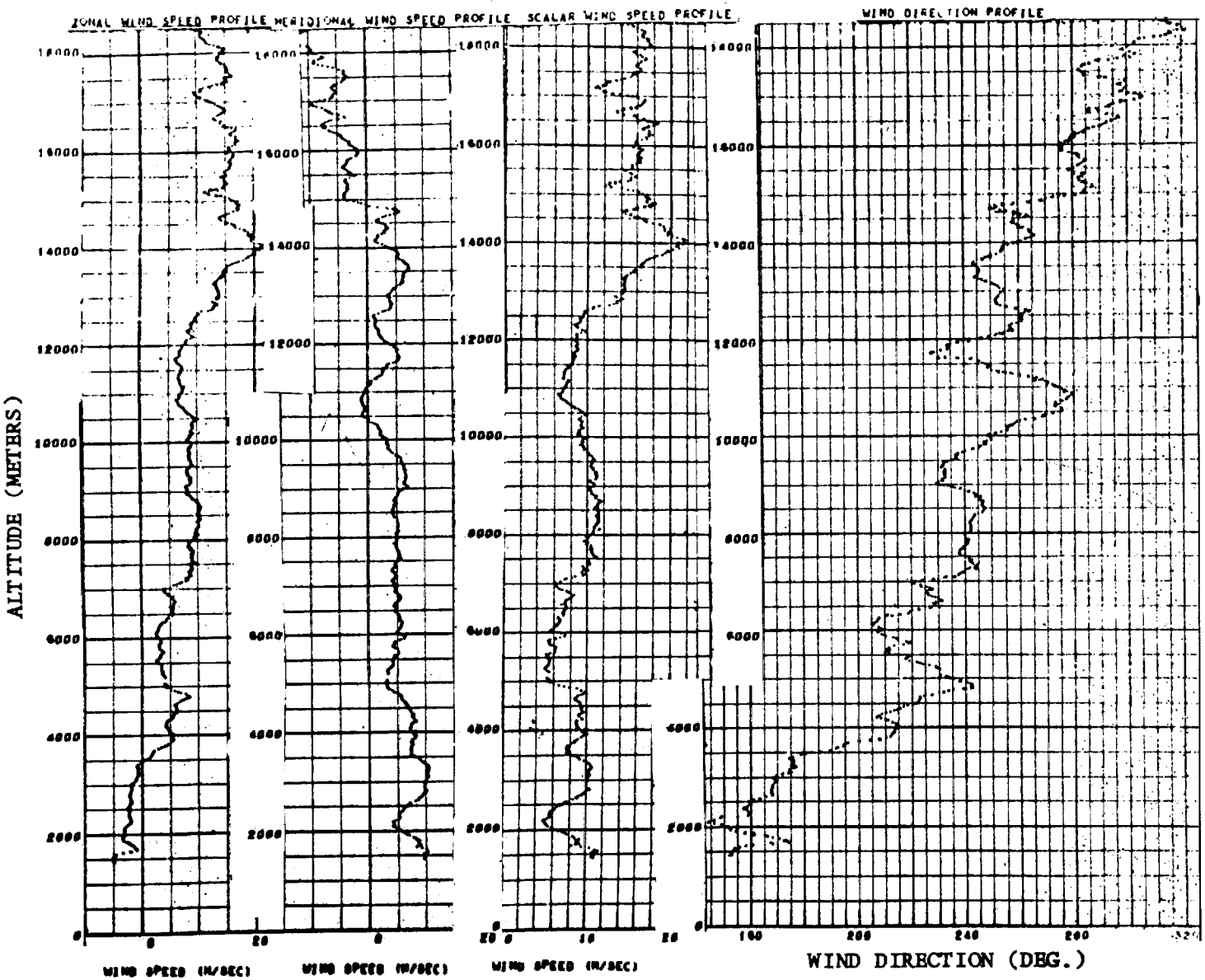

FIGURE 12 ZONAL, MERIDIONAL, SCALAR WIND SPEED PROFILE AND WIND DIRECTION AS DETERMINED BY FPS/16 RADAR TRACK OF A JIMSPHERE MODEL 3-7.5-398F

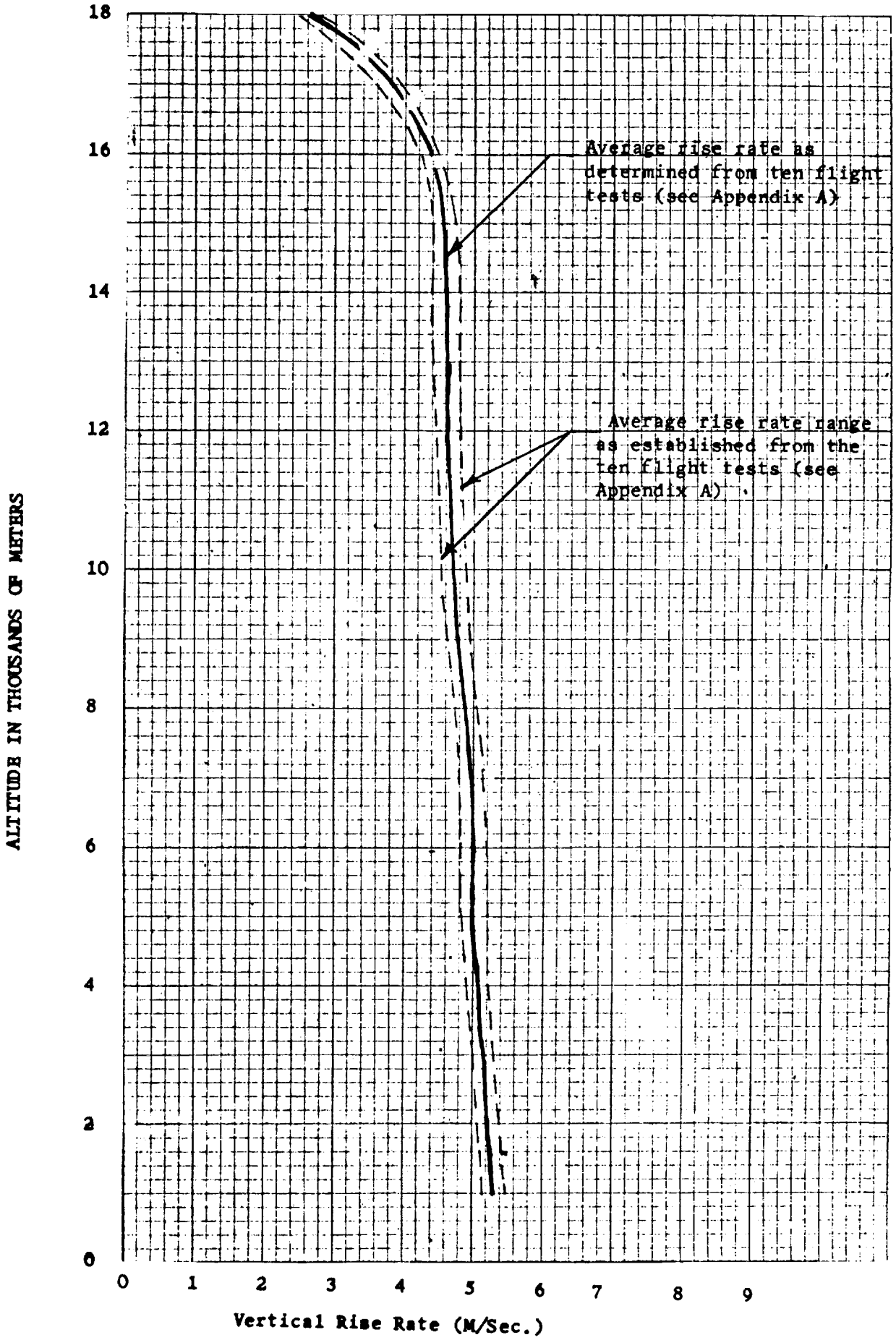

FIGURE 13 RISE RATE VERSUS ALTITUDE FOR THE JIMSPHERE MODEL 3-7.5-398F AS DETERMINED FROM FLIGHT DATA

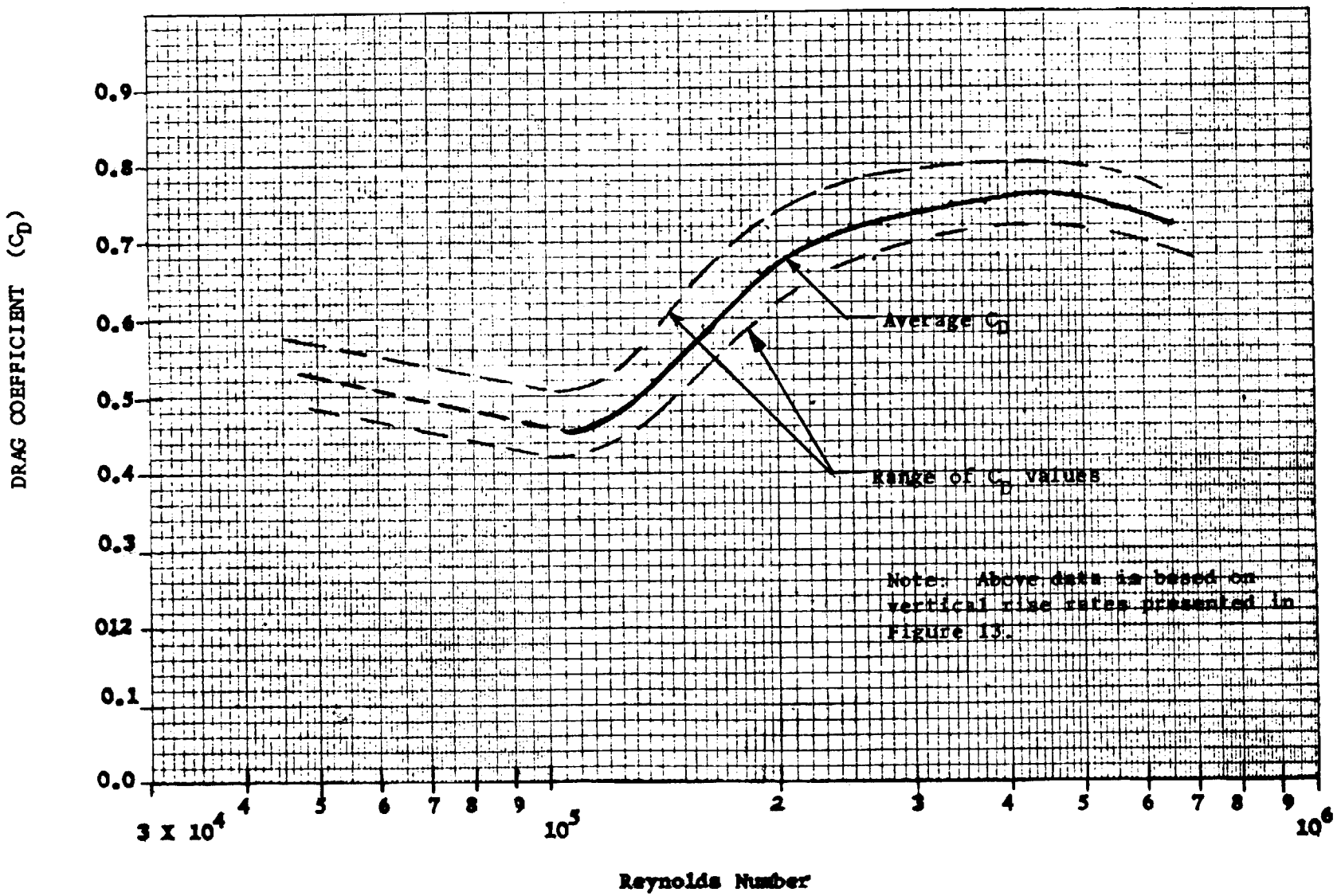

FIGURE 14 JIMSPHERE DRAG COEFFICIENT VERSUS REYNOLDS NUMBER AS DETERMINED FROM FLIGHT DATA

The drag coefficient values as determined from flight data are considerably greater than the values of drag coefficient determined by testing a model in a wind tunnel (see Section IV). No specific reason for this variation in drag coefficient can be given at this time, however the same condition was known to exist for the 2-meter diameter smooth spheres (Reference 5). MacReady and Jex (Reference 6) indicate that variations in drag can be expected with variations in Relative Mass of the sphere to the fluid it displaces.

IV. DERIVATION OF THE EQUATION OF MOTION FOR JIMSPHERE WIND SENSOR

The movement of an ascending balloon is governed by the equation of motion which may be written symbolically as:

$$\Sigma\bar{F} = (m_s + m_G) \frac{d}{dt} \bar{V}_B \qquad (1)$$

where

m_s = mass of balloon including accessories

m_G = mass of included gas

$\bar{V}_B$ = velocity of balloon

ΣF = sum of all external forces acting on the balloon.

The physical conditions are somewhat complicated when such a rising balloon enters a wind shear layer, schematically shown in Figure 15. In particular, three significant velocities may be identified; namely, the velocity of the balloon $\bar{V}_B$, the velocity of the air $\bar{V}_w$, and the relative velocity between the balloon and the surrounding air, $\bar{V}_R$.

Choosing Z as the vertical and X as the horizontal direction of movement, restricts the motion of the balloon to the X-Z plane. The velocity of the wind has then merely an X-component while the balloon velocity has X and Z components as schematically shown in Figure 16. One may write:

$$\bar{V}_w = V_{X_W} \hat{i} \qquad (2)$$

$$\bar{V}_B = V_{X_B} \hat{i} + V_{Z_B} \hat{k} \qquad (3)$$

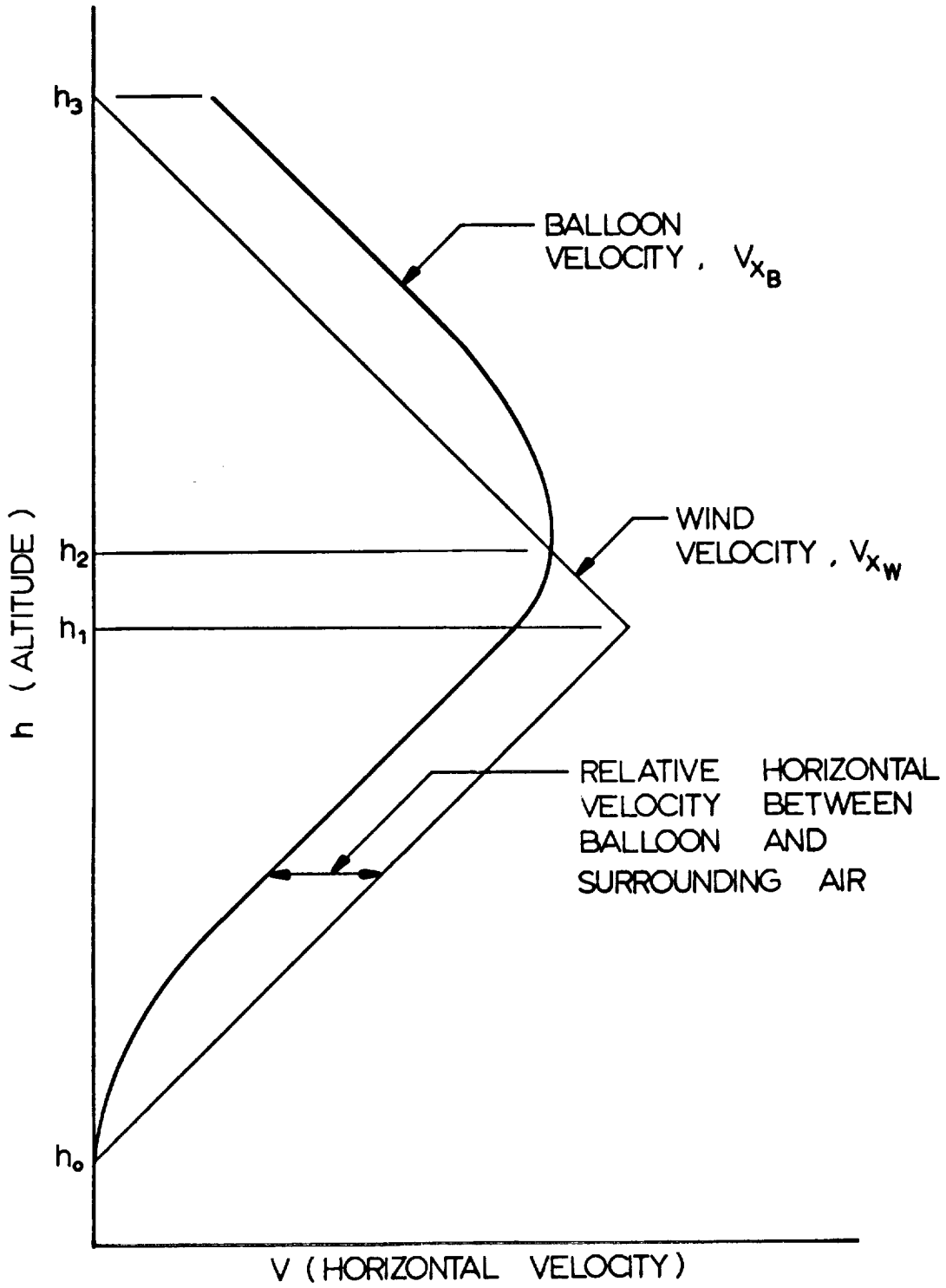

FIG 15. WIND SHEAR AND BALLOON VELOCITY AS A FUNCTION OF ALTITUDE

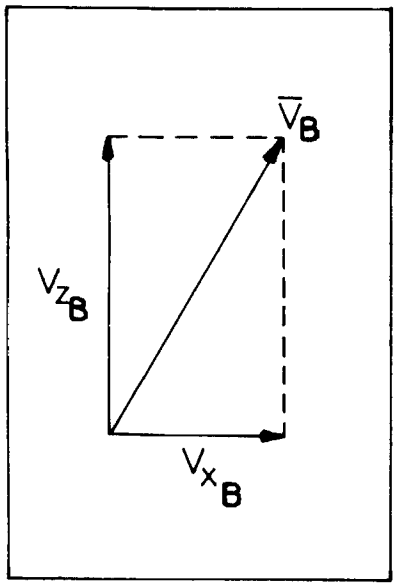

BALLOON VELOCITY

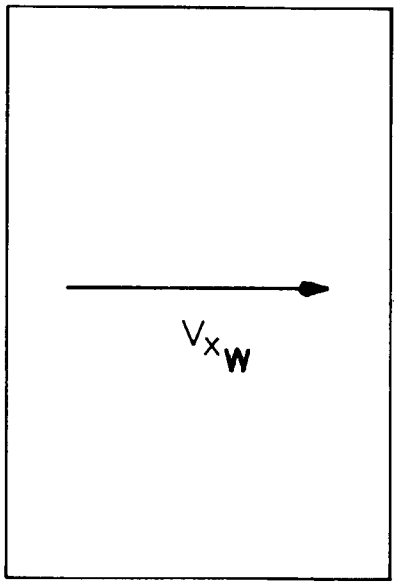

ABSOLUTE WIND VELOCITY

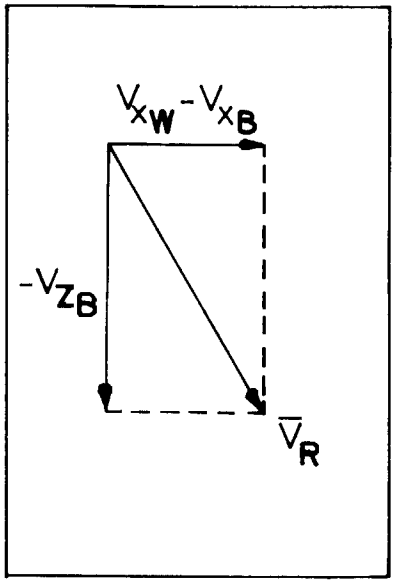

RELATIVE VELOCITY BETWEEN BALLOON AND SURROUNDING AIR

FIG 16 SCHEMATIC REPRESENTATION OF VARIOUS VELOCITIES

The velocity of the balloon with respect to the surrounding air is then

$$\bar{V}_R = (V_{X_W} - V_{X_B})\hat{i} - V_{Z_B}\hat{k} \tag{4}$$

The external forces acting on the balloon are the aerodynamic drag, gravity, buoyancy, and the apparent mass effect. Mathematically, these may be expressed respectively as:

$$\Sigma\bar{F} = \bar{D} + \bar{W} + \bar{B} + \bar{F}_A \tag{5}$$

The aerodynamic drag is expressed in conventional terms as

$$\bar{D} = C_D \frac{\rho}{2} V_R^2 S\, \hat{v} \tag{6}$$

where

$\hat{v} = \bar{V}_R / \left|V_R\right|$, the unit vector in the direction of the relative velocity.

Eliminating $\hat{v}$ from Eqn 6, one obtains

$$\bar{D} = C_D \frac{\rho}{2} V_R S\, \bar{V}_R \tag{7}$$

In view of Eqn (4), Eqn. (7) becomes:

$$\bar{D} = C_D \frac{\rho}{2} V_R S \left[(V_{X_W} - V_{X_B})\hat{i} - V_{Z_B}\hat{k}\right] \tag{8}$$

The gravity force is given by:

$$\bar{W} = -(m_s + m_G) g \hat{k} \tag{9}$$

The buoyancy force is given by the weight of air displaced by the balloon, thus:

$$\bar{B} = \rho g\ VOL.\hat{k} \tag{10}$$

where

VOL = volume of balloon

g = acceleration of gravity.

The effect of the apparent mass acts as a free force upon the object and is the result of the time rate of change of the momentum of the surrounding flow field. In this case, one obtains

$$\bar{F} = m' \dot{\bar{V}}_R$$

Since it was postulated that the balloon does not accelerate vertically, this equation reduces to:

$$\bar{F}_A = m'(\dot{V}_{X_W} - \dot{V}_{X_B})\hat{i} \tag{12}$$

Thus, the effect of the apparent mass is present in the horizontal direction only.

We can now write the summation of forces on the balloon

$$\Sigma\bar{F} = C_D \frac{\rho}{2} V_R S \left[(V_{X_W} - V_{X_B})\hat{i} - V_{Z_B}\hat{k} \right]$$
$$-(m_s + m_G)g\hat{k} + \rho g \, VOL.\hat{k} + m'(\dot{V}_{X_W} - \dot{V}_{X_B})\hat{i} \tag{13}$$

Substituting this relation and Eqn. 3 into Eqn. 1, yields

$$(m_s + m_G)(\dot{V}_{X_B}\hat{i} + \dot{V}_{Z_B}\hat{k}) =$$
$$C_D \frac{\rho}{2} V_R S \left[(V_{X_W} - V_{X_B})\hat{i} - V_{Z_B}\hat{k} \right]$$
$$-(m_s + m_G)g\hat{k} + \rho g \, VOL.\hat{k} \tag{14}$$
$$+m'(\dot{V}_{X_W} - \dot{V}_{X_B})\hat{i}$$

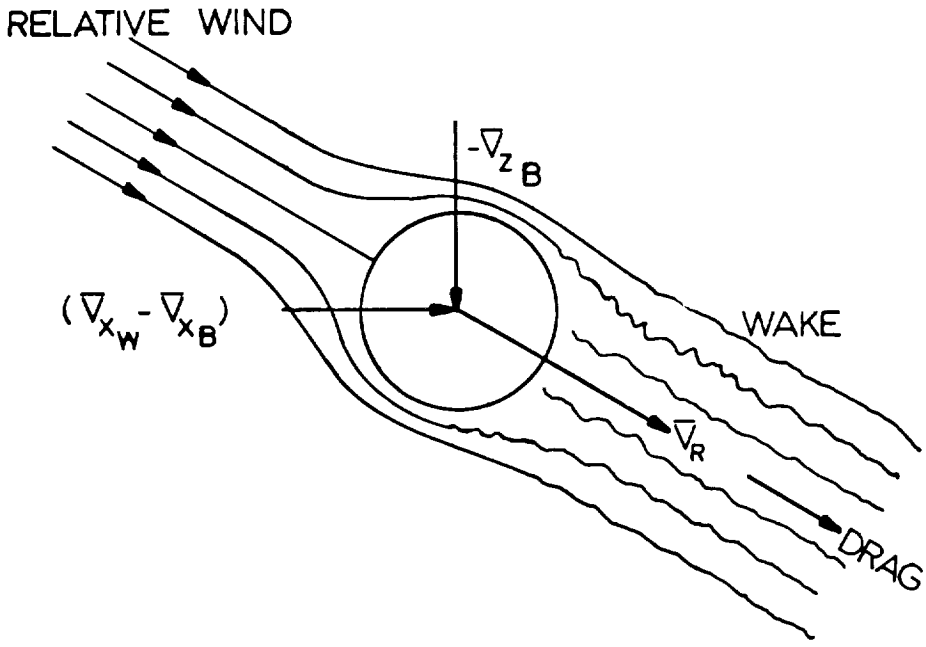

FIG 17. DRAG FORCE ON BALLOON BETWEEN ALTITUDES h_0 AND h_2

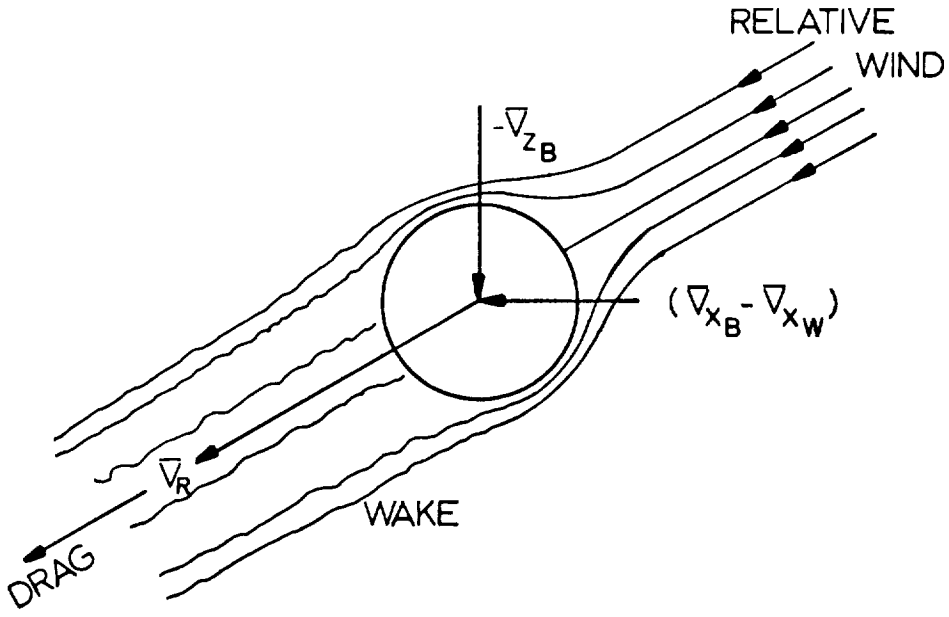

FIG 18. DRAG FORCE ON BALLOON BETWEEN ALTITUDES h_2 AND h_3

or, in terms of the horizontal and vertical component directions, respectively:

$$(m_s+m_G)\dot{V}_{X_B} = C_D\frac{\rho}{2}V_R S(V_{X_W} - V_{X_B}) + m'(\dot{V}_{X_W}-\dot{V}_{X_B}) \tag{15}$$

and

$$(m_s+m_G)\dot{V}_{Z_B} = -C_D\frac{\rho}{2}V_R S V_{Z_B} - (m_s+m_G)g + \rho g \text{ VOL.} = 0 \tag{16}$$

Equation 14 represents the general equation of motion of a rising balloon. The physical meaning of this equation shall now be discussed in view of the balloon rise rate and wind shear conditions shown in Figure 15.

As illustrated, the wind velocity increases between h_o and h_1, while the balloon velocity also increases, but because of the necessary acceleration always remains smaller than the wind velocity. Therefore, in this altitude region, one may write:

$$V_{X_W} > V_{X_B} \tag{17}$$

and also in general

$$\dot{V}_{X_W} > \dot{V}_{X_B} \tag{18}$$

At the altitude h_1, the wind velocity begins to decrease at a constant rate and its time rate of change as experienced from the rising balloon becomes negative. However, over a certain distance, the wind continues to move faster than the balloon until the relative

velocity between the balloon and wind approaches zero towards the altitude h_2.

Therefore, one observes that for the region of $h_1 < h < h_2$, the wind velocity is higher than the balloon velocity while for the same region of $V_{X_W} > V_{X_B}$, the rate of change of the wind is stronger than that of the balloon, and one may write $\dot{V}_{X_W} < \dot{V}_{X_B}$.

Finally one observes that the balloon is as fast as the wind at the altitude where $h = h_2$, and one obtains $V_{X_W} = V_{X_B}$.

After the balloon passes h_2, its velocity becomes greater than the wind velocity and the balloon decelerates at least for a part of the trajectory at a slower rate than the time rate of change of the wind. Therefore, the rate of change of wind velocity in this region is also stronger negative than that of the balloon and one observes for $h_2 < h < h_3$ that

$$V_{X_W} < V_{X_B} \tag{19}$$

and also

$$\dot{V}_{X_W} < \dot{V}_{X_B} \tag{20}$$

These changes of flow patterns and the related consequences are schematically shown in Figures 17 and 18.

In view of the above explanations it can be seen that the aerodynamic drag and the effects of apparent mass may accelerate or decelerate the balloon, depending on the particular zone of the wind shear layer. Details of these effects are schematically shown in

Table I, and these conditions will have to be considered in calculations of the balloon's flight path and its wind response error.

TABLE 1

ACTION OF AERODYNAMIC DRAG AND EFFECT OF APPARENT MASS UPON A RISING BALLOON IN A WIND SHEAR LAYER

REGION	$V_{X_W} - V_{X_B}$	$\dot{V}_{X_W} - \dot{V}_{X_B}$	AERODYNAMIC DRAG	EFFECT OF APPARENT MASS
$h_o > h_1$	> 0	> 0	Accelerating	Accelerating
$h_1 > h_2$	> 0	< 0	Accelerating	Decelerating
h_2	0	< 0	0	Decelerating
$h_2 > h_3$	< 0	< 0	Decelerating	Decelerating

V. JIMSPHERE WIND TUNNEL DRAG COEFFICIENT MEASUREMENTS

A. Procedure

Wind tunnel studies to determine the drag coefficient of a 3-7.5-398F Jimsphere for various Reynolds numbers were conducted in the subsonic wind tunnel of the University of Minnesota. Identical experiments were made on a smooth sphere in order to compare the respective drag coefficients.

Figure 19 shows the 5-inch diameter Jimsphere model in the wind tunnel, suspended by means of a sting. The drag measuring element was mounted between the vertical strut and the sting. It consisted of a standard strain gage bridge circuit glued to elastic cantilever beams. The amplified output of the drag element was recorded on a Honeywell Visicorder. The Reynolds number of the experiments was varied from 70,000 to 400,000 by changing the velocity.

B. Models

Two 5-inch diameter hard rubber spheres were used as models in the drag coefficient studies. Both spheres had 1/2-inch threaded holes for sting attachment. One sphere remained smooth, the other was used for the scale model of a 3-7.5-398F Jimsphere (Figure 20). In constructing the Jimsphere model, scale gore patterns showing the position of the projections were made, and fastened to the sphere. The sphere was then mounted in an indexing jig of a vertical milling machine with a rotating head. Then, setting the head of the milling machine to the calculated angle

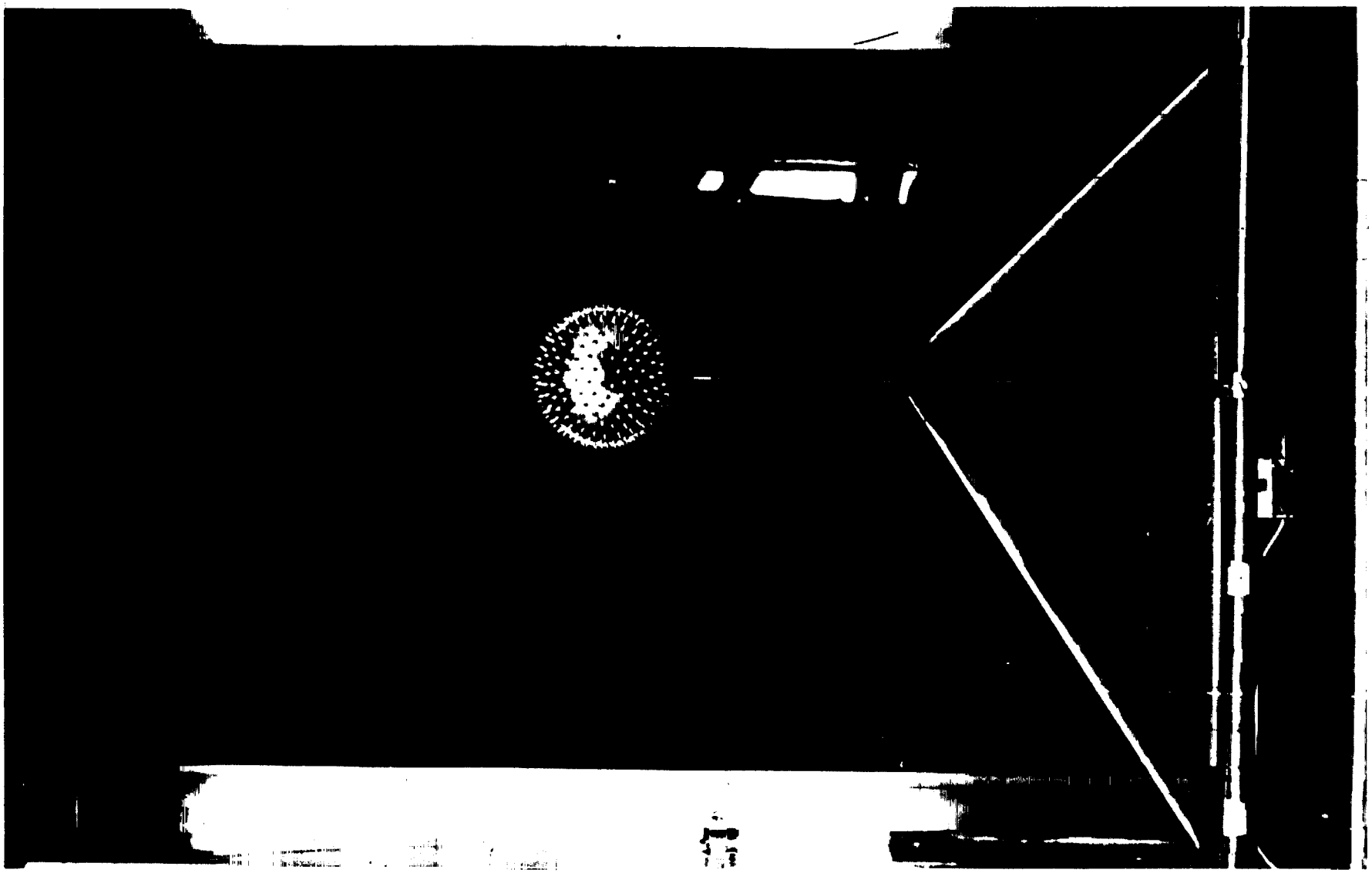

FIG 19. MODEL JIMSPHERE MOUNTED IN WIND TUNNEL

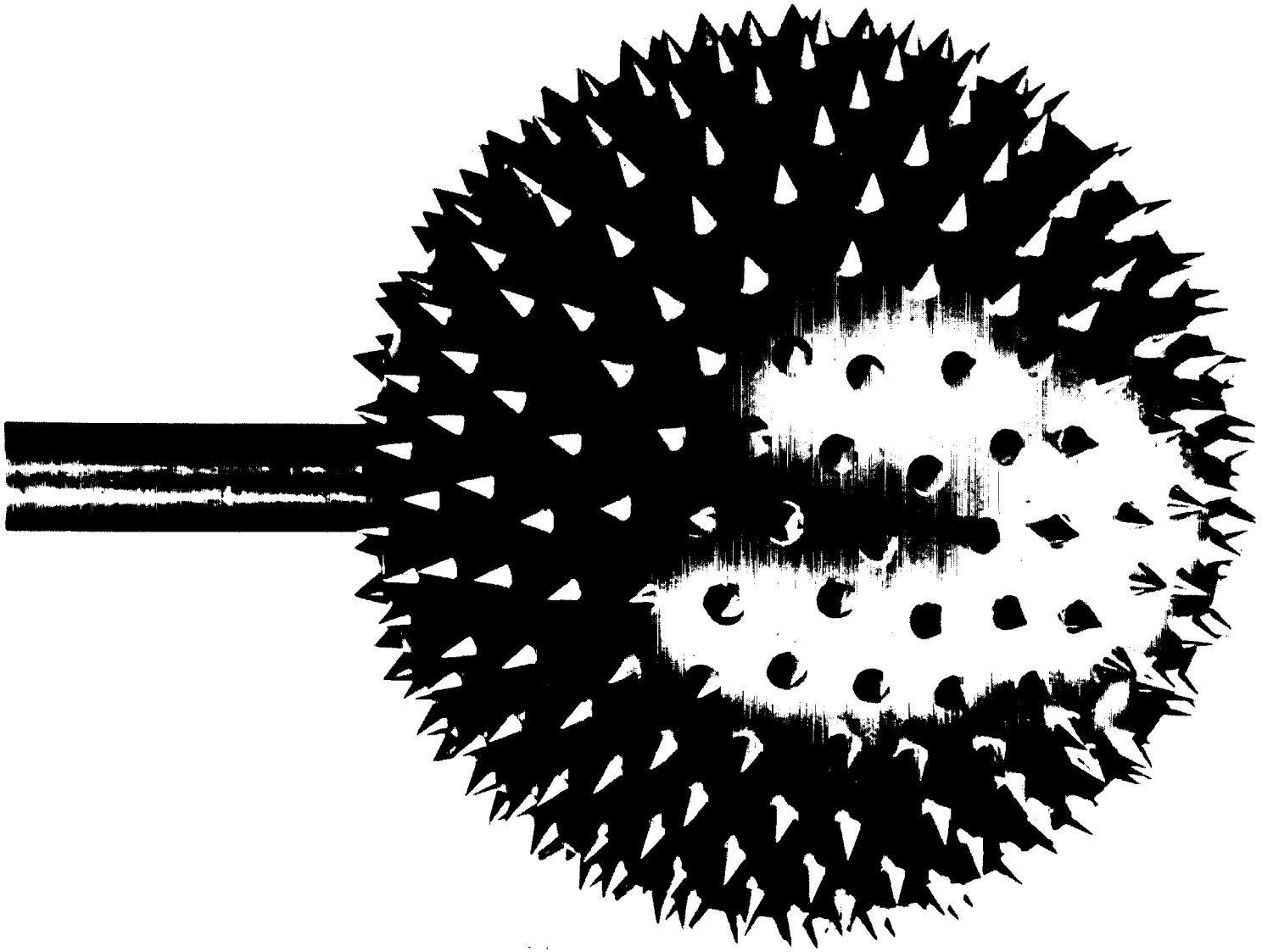

FIG 20. JIMSPHERE MODEL USED IN WIND TUNNEL TESTS

between an individual projection and the sting axis of the sphere, the holes for the projections were drilled. The conical projections were machined from 3/16-inch diameter brass rod, and inserted in the previously drilled holes on the sphere.

C. Results

The drag coefficients of the 3-7.5-398F Jimsphere and the smooth sphere are plotted versus Reynolds number in Figure 21. The sphere drag coefficients have been corrected for wind tunnel turbulence (Reference 10); no correction was used for the Jimsphere drag coefficients. It is evident that within the Reynolds number range (100,000 to 500,000) the drag coefficient of the Jimsphere changes very little, while the smooth sphere has the characteristic variation of drag coefficient. The wind tunnel measurements indicate that the drag coefficient of a Jimsphere is relatively insensitive to Reynolds number changes in the range where a smooth sphere has the classical variation. The drag coefficient of the Jimsphere is somewhat smaller than the drag coefficient of the smooth sphere in the subcritical Reynolds number region.

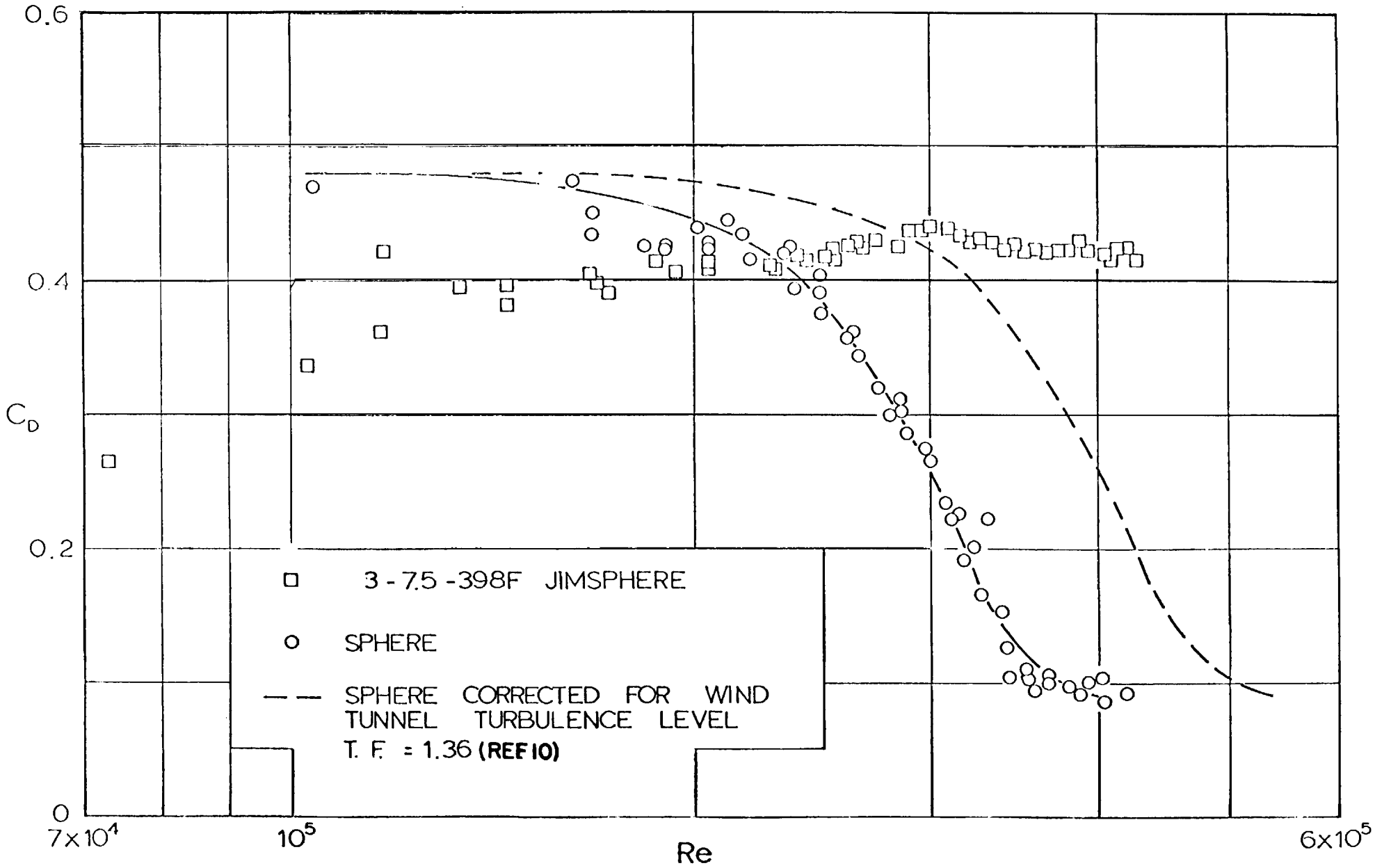

FIG. 21 DRAG COEFFICIENT VS. REYNOLDS NUMBER FOR A JIMSPHERE AND A SMOOTH REFERENCE SPHERE.

VI. JIMSPHERE APPARENT MASS TESTS

A. Procedure

The equation of motion of a balloon rising through a wind shear includes terms representing the effect of the apparent mass of the balloon. Theoretical and experimental values of apparent mass for smooth spheres are available but the apparent mass of a roughened sphere such as the Jimsphere had not heretofore been determined. Therefore, experiments were made at the University of Minnesota, with the objective to determine characteristic values representing the apparent mass of the 3-7.5-398F and 4-8-290F Jimsphere balloons.

Two full-size Jimsphere balloons were tested using the procedure illustrated in Figure 22, which has been used previously for smooth spherical balloons (Reference 7) and parachutes.

The balloons, equipped with an accelerometer, were dropped from a height of about 25 ft., and a known weight suspended beneath the balloon, the lost weight, W_L, was allowed to strike the floor. Since the drag on the balloon remains nearly constant just after impact of the lost weight, the balloon deceleration becomes merely a function of the change of mass of the system.

However, in most cases the balloon system did not fully achieve a steady state condition before impact. Therefore, the acceleration just prior to impact also had to be considered.

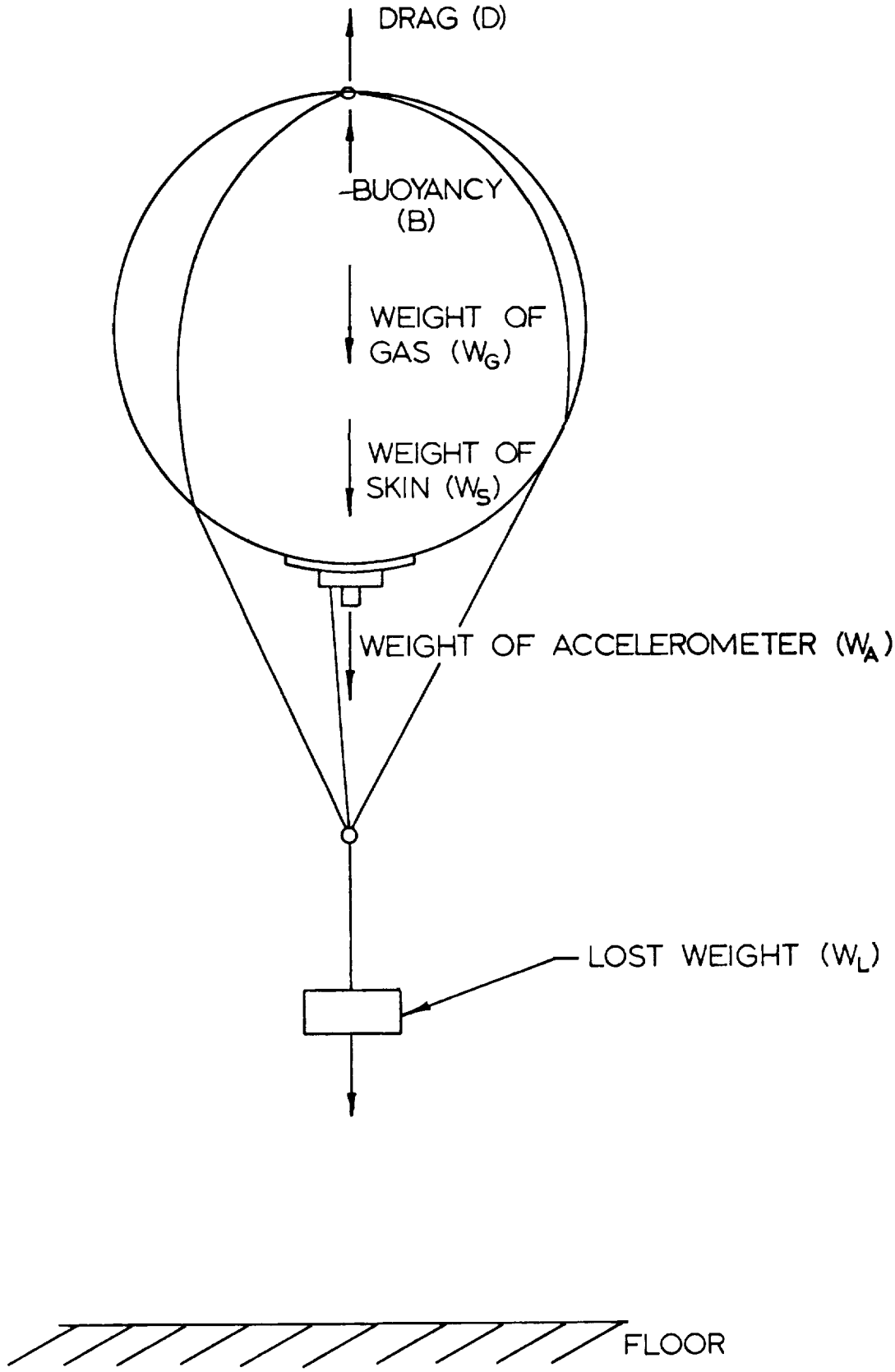

FIG 22 FORCES ACTING ON THE EXPERIMENTAL SYSTEM DURING DESCENT

The equation of motion of the balloon system before the lost weight strikes the ground is (Figure 22):

$$W_R + W_L - B - D = \left(\frac{W_R + W_L + W'}{g}\right) a. \qquad (1)$$

After impact, the equation of motion is:

$$W_R - B - D = \left(\frac{W_R + W'}{g}\right) a \qquad (2)$$

in which W_L and W_R represent "Lost" and "Remaining" weight, respectively, while "a" represents acceleration, W' apparent mass, and B and D bouyancy and drag. With the notations $n_o = a_o/g$ and $n = a/g$, and assuming that the drag remains constant just before and just after impact, Equations 1 and 2 can be combined and rearranged to yield:

$$W' = \frac{W_L(1 - n_o)}{n_o - n} - W_R \qquad (3)$$

The accelerations n_o and n were obtained from the accelerometer mounted on the balloon. The remaining weight, W_R, was determined using the static weight of the balloon system and the bouyancy,

$$W_R = W_n - W_L + B \qquad (4)$$

In order to obtain the bouyancy using

$$B = \rho\, g\, VOL. \qquad (5)$$

the volume of each balloon was determined by measuring the time needed to fill the balloon from a regulated air supply. Atmospheric pressure and temperature were measured during the tests so the

atmospheric density could be calculated from the perfect gas law.

B. Models

The experimental system for apparent mass measurements consisted of a balloon, balloon rigging and accelerometer, and data recording equipment.

1. Balloons

Four helium-filled Jimsphere balloons were used in the apparent mass studies. Two balloons were 3-7.5-398F Jimspheres and two were 4-8-290F Jimspheres (Figure 23). All were constructed of 1/2 mil Mylar with 12 gores, and the basic spheres were about 2 meters in diameter. The balloon systems without the lost weight, W_L, had a net lift of about 2 lbs., and a lost weight of about 3 lbs. was used.

3. Balloon Rigging and Accelerometer

Since the Jimsphere balloons had skin thicknesses only 1/8 that of the spherical balloons previously tested, the vibration of the spherical bodies which were recorded by the accelerometer and which are generated due to the impact of the lost weight, was considerably increased. To reduce this vibration various arrangements and numbers of suspension lines, with different damping systems between the balloon and the accelerometer, were tried, but with little success. The best suspension system was that used

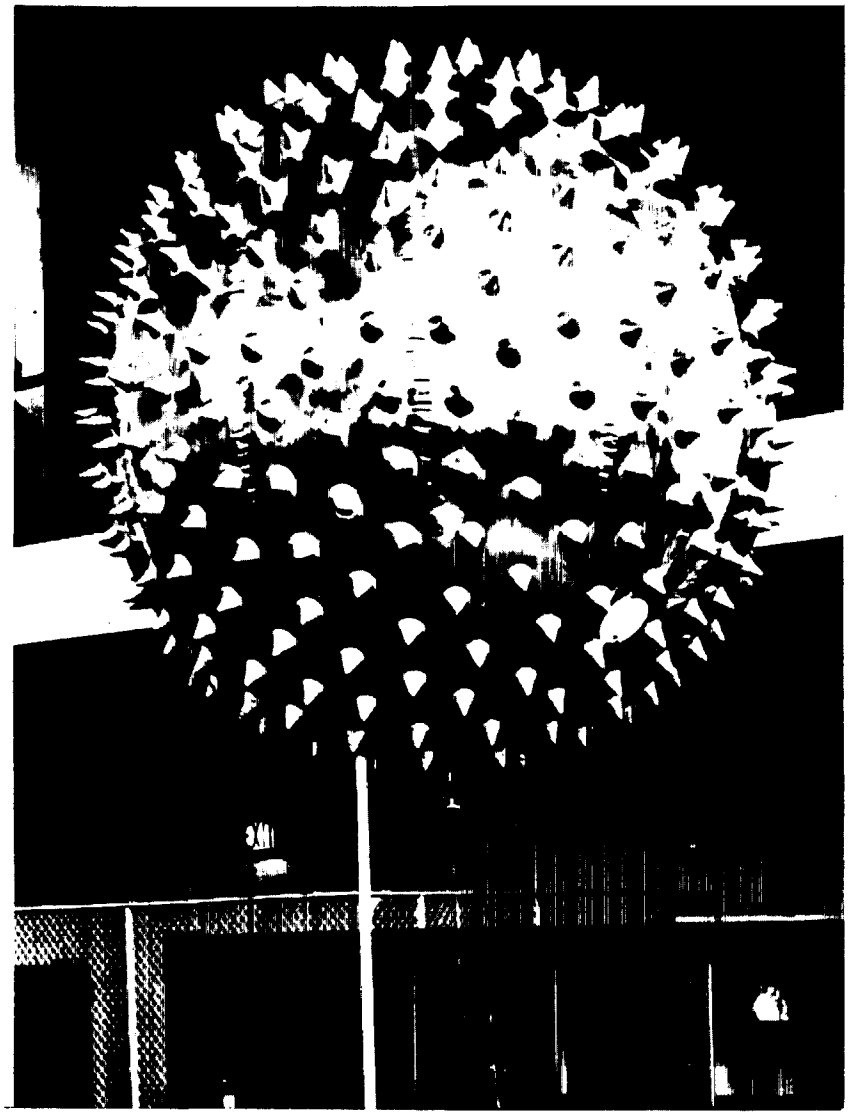

A) MODEL 3-7.5-398F

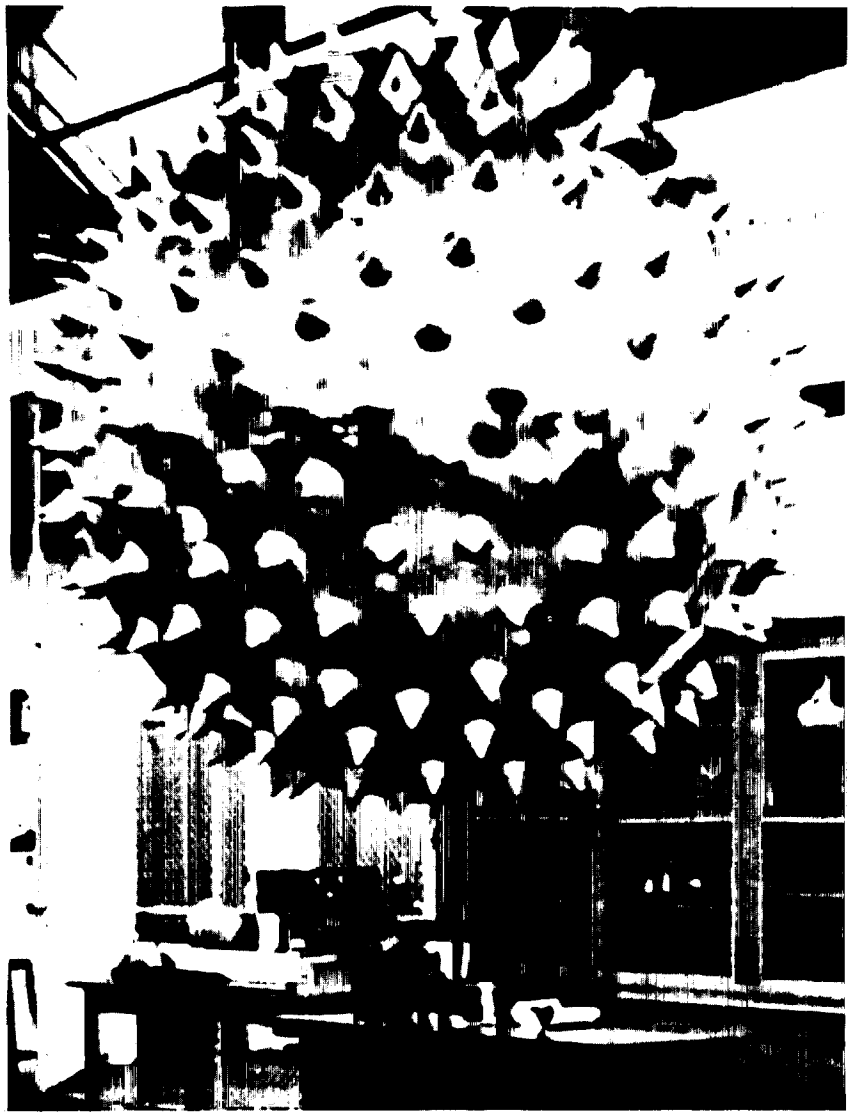

B) MODEL 4-8-290F

FIG 23 JIMSPHERE BALLOONS

in the previous tests (Reference 7).

The balloon rigging system consisted of three 0.017-inch steel cables, equally spaced over the balloon surface, fastened together at the top and meeting at a confluence point below the balloon. This line system carried the lost weight.

A Statham accelerometer with a range of $\pm$ 3 g's was used to measure the accelerations of the balloon system. The accelerometer was fastened to an aluminum plate of 14-inch diameter, spherically curved and attached to the base of the balloon.

3. Data Recording

The amplified accelerometer output was recorded on a Honeywell Visicorder. A tracing of a recording of a typical experiment is shown in Figure 24. The vibration of the accelerometer both before and after the impact of the lost weight has been averaged out in the data reduction process.

C. Results

Each of the Jimsphere models was tested approximately 30 times in order to statistically minimize individual errors in measuring balloon system accelerations. Histograms of the apparent mass factor , K, (K = m'/B) for 3-7.5-398F and

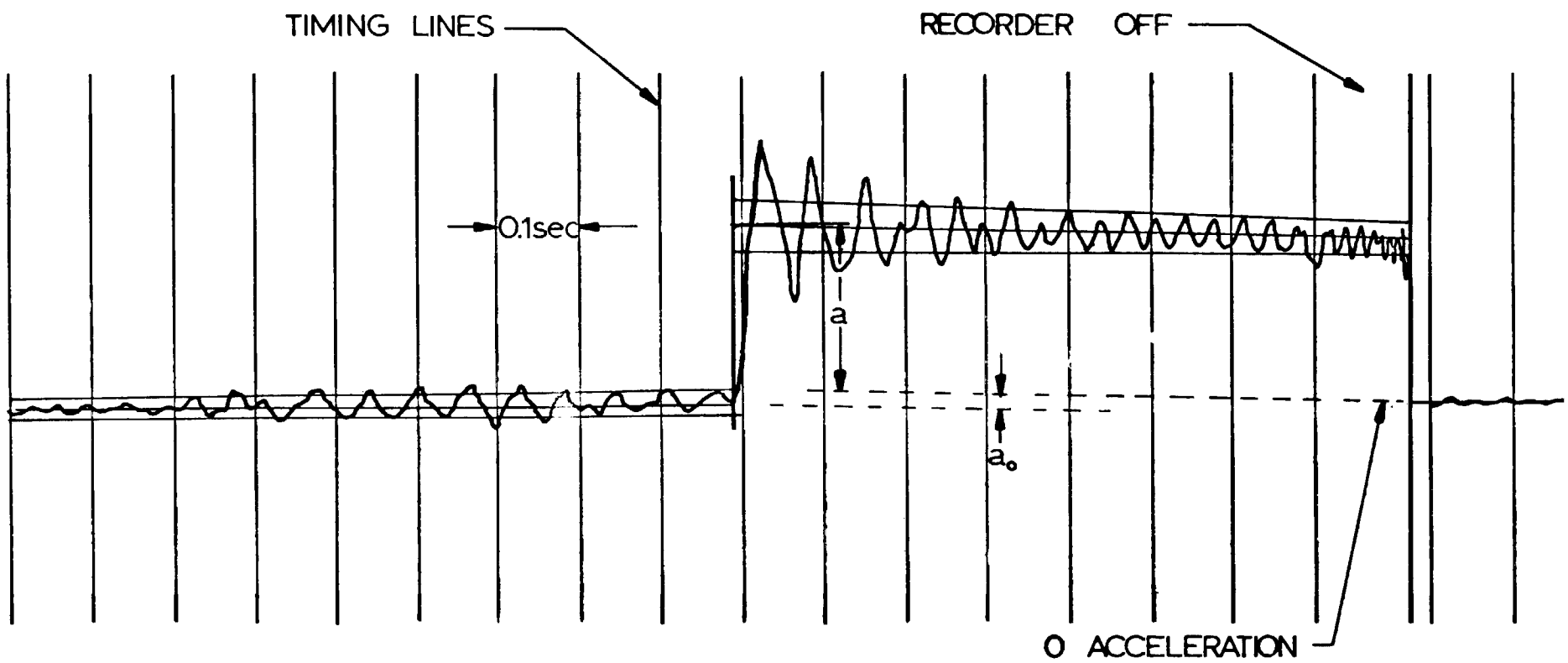

FIG 24 TYPICAL ACCELERATION VS TIME RECORDING OF A JIMSPHERE BALLOON

4-8-290F Jimspheres are shown in Figures 25 and 26, respectively.

These histograms show that neither distribution is normal and hence the arithmetic average is not necessarily the most probable value of K. By forming upper and lower bounds that include the most probable values of K in the drop tests, the range of variation in K is obtained. These values for the two Jimsphere models are:

Jimsphere Model	Average K	Range of Probable Values for K
3-7.5-398F	0.51	$0.46 \leqslant K \leqslant 0.58$
4-8-290F	0.59	$0.54 \leqslant K \leqslant 0.64$

This variation in the value of K is considerably greater than the experimental error involved in the test program. Also, the larger number of data points on either side of the average K value suggests that the apparent mass may not be single-valued, but rather a multi-valued function somewhat dependent upon wake formation, turbulence level, and physical characteristics of the balloon. The Reynolds number at which these values were obtained amounts to approximately $R_e = 300{,}000$.

The values of K = 0.51 and 0.59 are suggested to be considered as average and characteristic values.

It is interesting to note that the apparent mass of the Jimsphere with fewer but larger cones is higher than that of the

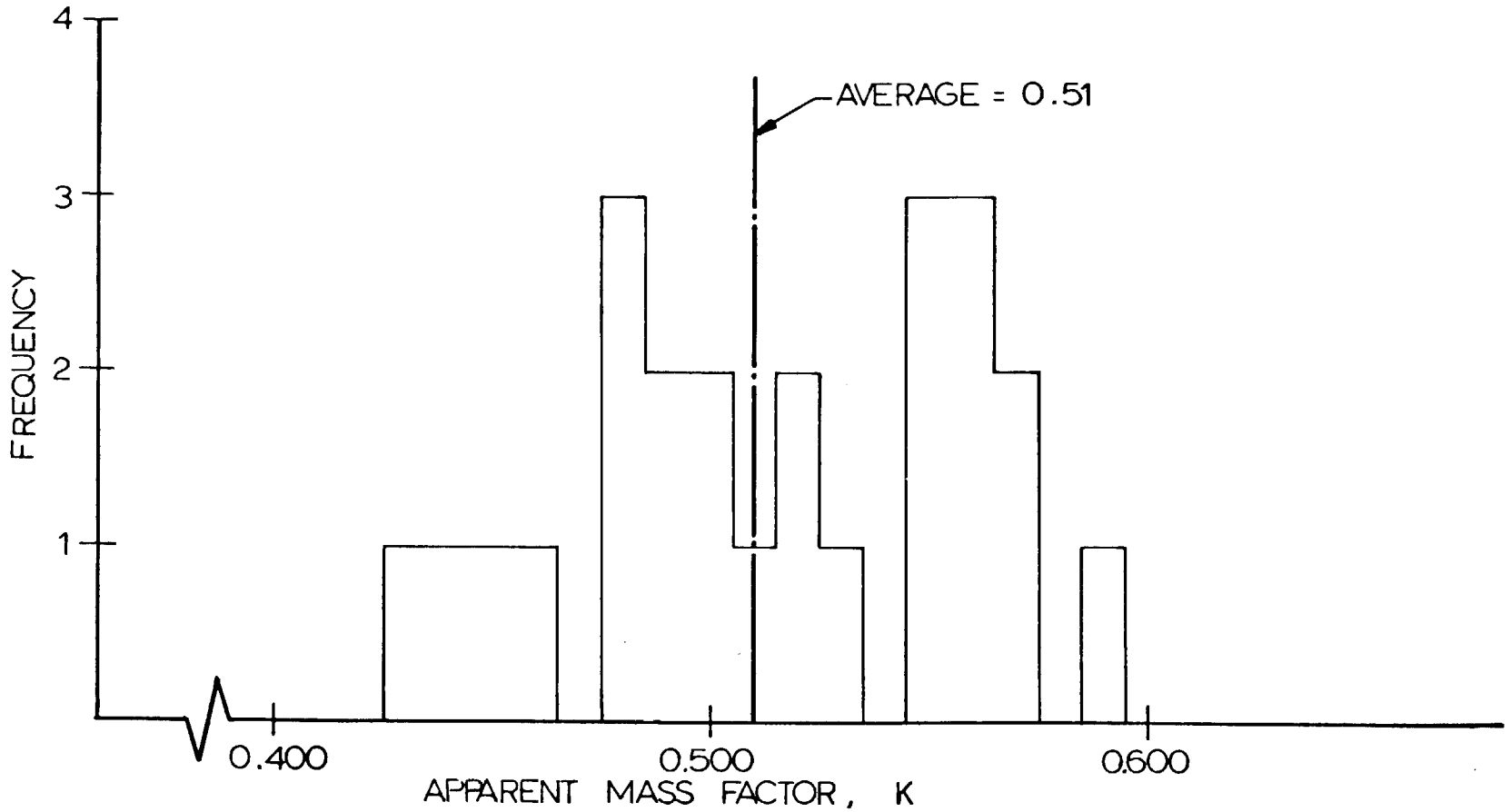

FIG 25 STATISTICAL FREQUENCY DISTRIBUTION OF THE APPARENT MASS FACTOR FOR THE 3-7.5-398F JIMSPHERE BALLOON

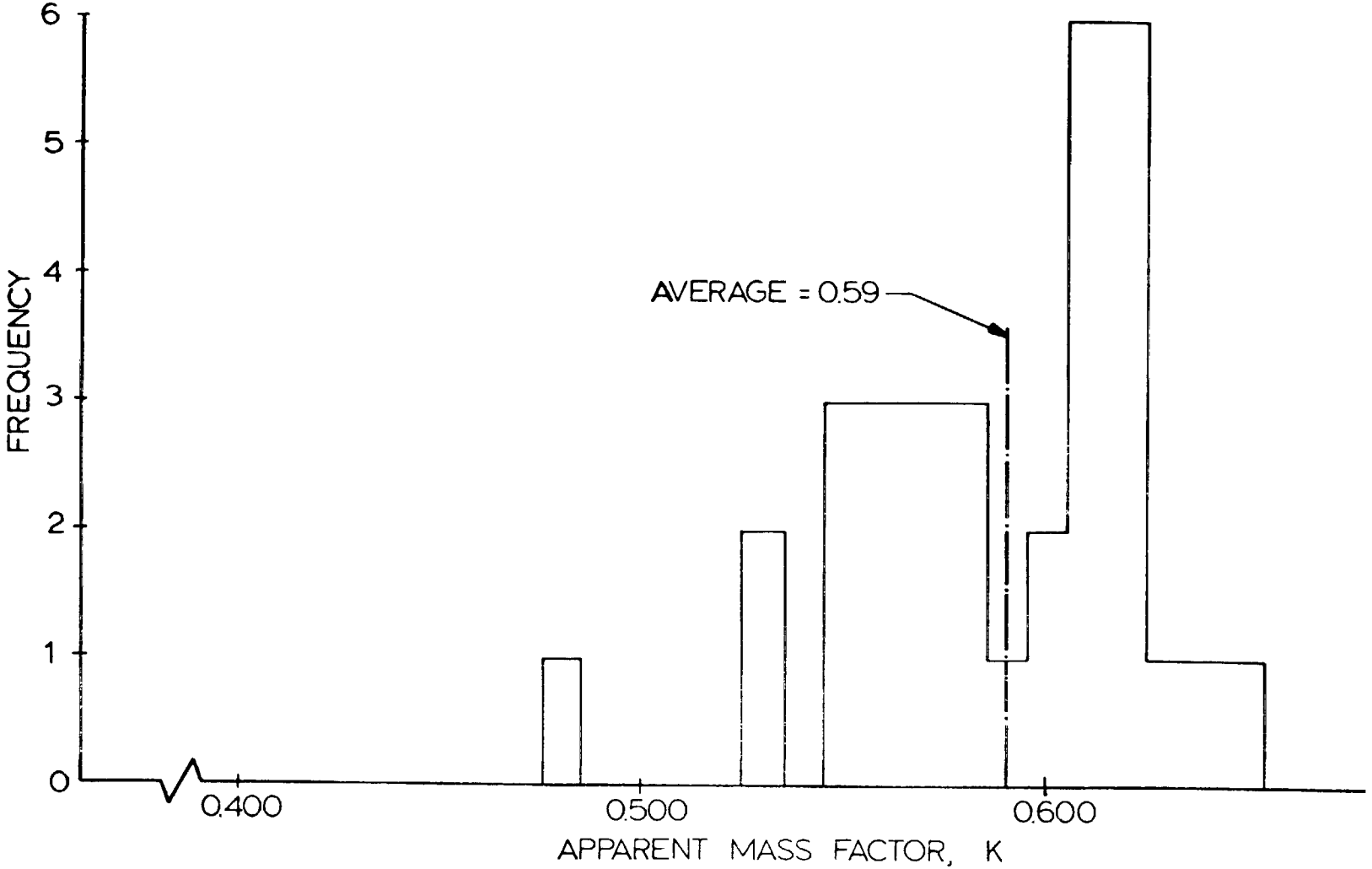

FIG 26 STATISTICAL FREQUENCY DISTRIBUTION OF THE APPARENT MASS FACTOR FOR THE 4-8-290F JIMSPHERE BALLOON

sphere with smaller cones. Furthermore, it appears that the apparent mass of the Jimsphere is, in general, slightly higher than the apparent mass of a comparable smooth sphere.

VII. WIND RESPONSE CAPABILITIES OF THE JIMSPHERE

A. Wind Response Error

The wind response capabilities of the Jimsphere can best be presented by indicating the magnitude of the wind response error or velocity lag ($V_{X_W} - V_{X_B}$) of the Jimsphere for any given wind gradient condition. The magnitude of the wind response error ($V_{X_W} - V_{X_B}$) for a wind gradient condition can be determined from a solution of the equations of motion for the Jimsphere based on the following assumptions:

1. The wind gradient is constant over the altitude interval under consideration.
2. The wind gradient is not of such magnitude to cause a change in the balloon rise rate (α = 0.28 per second or less) (Reference 8).

The equations of motion as presented in the previous section are:

X (horizontal)

$$(m_s+m_G)\dot{V}_{X_B} = C_D\tfrac{1}{2}\,\rho S V_R (V_{X_W} - V_{X_B}) + m' (\dot{V}_{X_W} - \dot{V}_{X_B}) \qquad (1)$$

Z (vertical)

$$(m_s+m_G)\dot{V}_{Z_B} = -C_D\tfrac{1}{2}\,\rho V_R V_{Z_B} S - (m_s+m_G)\, g + \rho g\ VOL \qquad (2)$$

Based on assumption 2,

$\dot{V}_{Z_B} = 0$, and equation (2) can be rearranged to

$$V_R = \frac{\rho g\ VOL - (m_s+m_G)\, g}{C_D\tfrac{1}{2}\,\rho S\ V_{Z_B}} \qquad (3)$$

For constant wind gradients

$$\dot{V}_{X_W} = \frac{dV_{X_W}}{dh} \qquad \frac{dh}{dt} = \alpha V_{Z_B} \tag{4}$$

$$\text{and } V_{X_W} = V_{X_{W_o}} + \alpha(h - h_o) \tag{5}$$

In addition

$$\dot{V}_{X_B} = \frac{dV_{X_B}}{dh} \qquad \frac{dh}{dt} = \frac{dV_{X_B}}{dh} \quad V_{Z_B} \tag{6}$$

Substituting equations (3), (4), (5) and (6) into equation (1) and solving the resulting differential equation (detailed derivation presented in Appendix B) we find that the wind response error is

$$V_{X_W} - V_{X_B} = (V_{X_W} - V_{X_B})_o \; e^{-\frac{(h-h_o)}{R}} + \alpha L \left[1 - e^{-\frac{(h-h_o)}{R}}\right] \tag{7}$$

Where L = Lag distance

$$L = \left[\frac{(m_s + m_G)}{\rho VOL - (m_s + m_G)}\right] \frac{V_{Z_B}^2}{g} \tag{8}$$

and R = Response length

$$R = \left[\frac{(m_s + m_G + m')}{\rho VOL - (m_s + m_G)}\right] \frac{V_{Z_B}^2}{g} \tag{9}$$

It should be noted that the lag distance (L) is not a function of the balloon apparent mass whereas the response length (R) is a function of apparent mass effects. In addition the effects of apparent mass reduce the velocity lag ($V_{X_W} - V_{X_B}$) during the period of response to the wind gradient condition. An illustration of lag distance (L) and response length (R) is given in Figure 27.

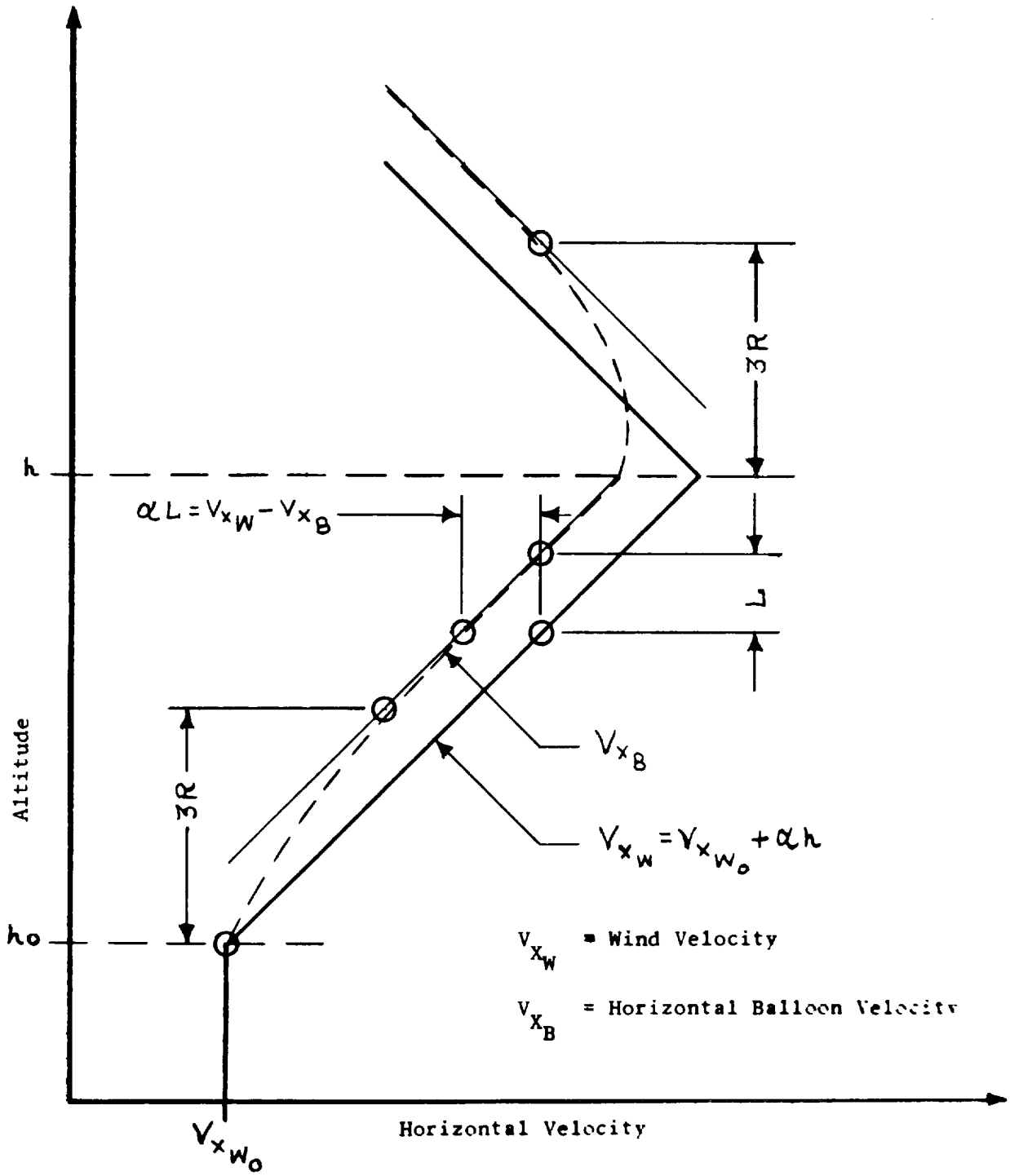

Figure 27 Illustration of Balloon Response Coefficients

B. Lag Distance

The lag distance (L) is a characteristic coefficient of a wind sensor, having the dimensions of length, which defines the capability of the sensor to indicate changing wind velocities. The shorter the lag distance (L) the better the wind sensor indicates actual wind velocities. The velocity lag ($V_{X_W} - V_{X_B}$) of the sensor is proportional to the product of the wind gradient (α) and the lag distance (L).

The ratio of the mass displaced by the balloon to the mass of the balloon system can be specified as a mass ratio (μ) as defined by equation (10).

$$\mu = \frac{\rho \text{ VOL}}{m_S + m_G} \quad \frac{\text{(Displaced Mass)}}{\text{(Displacement Mass)}} \tag{10}$$

Substituting equation (10) into equation (8) results in a presentation of the lag distance (L) as a function of mass ratio (μ), rise rate (V_{Z_B}), and the gravitational constant (g) (Reference 9) as shown in equation (11).

$$L = \frac{V_{Z_B}^2}{g}\left[\frac{1}{\mu-1}\right] \tag{11}$$

If is assumed that horizontal velocity errors ($V_{X_W} - V_{X_B}$) are small in relation to the vertical rise rate (V_{Z_B}) then equation (3) can be rewritten as

$$\rho g \text{ VOL} - (m_S + m_G)g = C_D \tfrac{1}{2} \rho S V_{Z_B}^2 \tag{12}$$

Substituting equation (12) into equation (8) and relating sphere volume (VOL) and cross sectional area (S) we have the lag distance (L) as a function of balloon diameter (Dia.), drag coefficient (C_D), rise rate (V_{Z_B}), and the gravitational constant (g) (Reference 9) as shown in equation (13).

$$L = \frac{4\ (\text{Dia.})}{3\ C_D} - \frac{V_{Z_B}^2}{g} \qquad (13)$$

The lag distance (L) of the Jimsphere at various altitudes is presented in Figure 28 as a function of mass ratio (μ) and in Figure 29 as a function of diameter (Dia.) and drag coefficient (C_D). In both Figures 28 and 29 the average Jimsphere rise rate as determined from analysis of flight tests and presented in Figure 13 was used in determining lag distances (L). The change in the shape of the lag distance (L) curve at higher altitudes is attributed to the fact that the vertical velocity decreases rapidly after 16,000 meters altitude and the Drag Coefficient is increasing.

The maximum velocity lag of the Jimsphere, ($V_{X_W} - V_{X_B}$), can be found by multiplying the Jimsphere lag distance (L) by the wind gradient (α). Figure 30 presents the velocity lag of the Jimsphere as a function of wind gradient (α) for several altitude conditions. A study of several balloon soundings indicates that wind gradients in excess of 0.1 per second are extremely rare. Below 12,000 meters altitude the maximum wind response error of

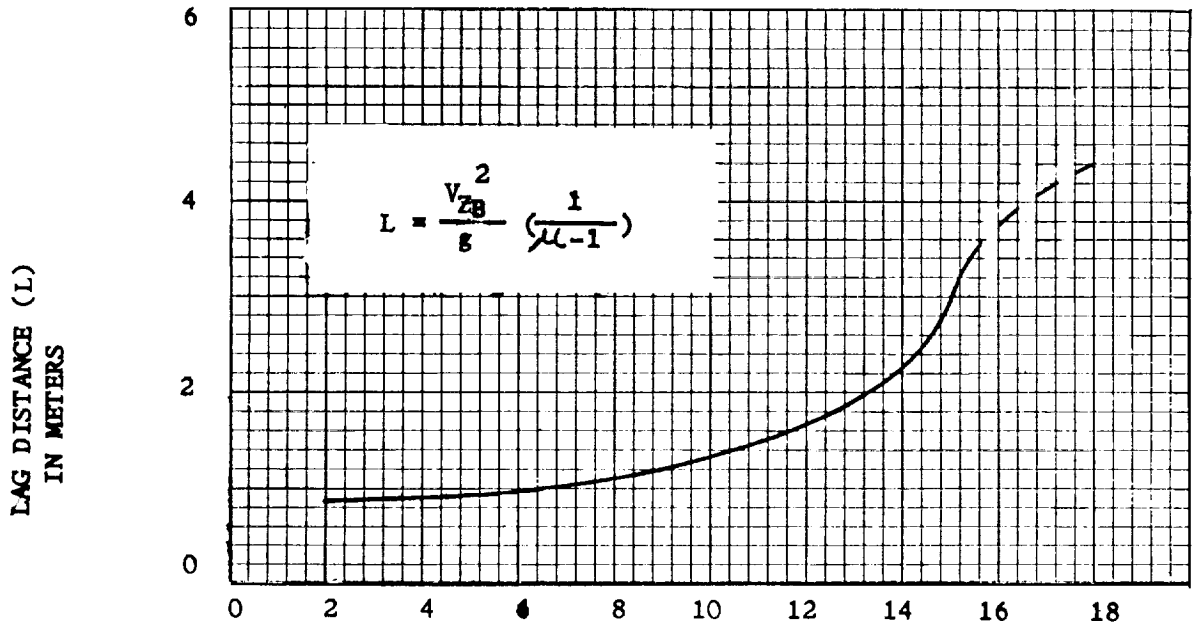

FIGURE 28 LAG DISTANCE (L) OF THE JIMSPHERE (BASED ON DRAG COEFFICIENT AND DIAMETER) AS A FUNCTION OF ALTITUDE

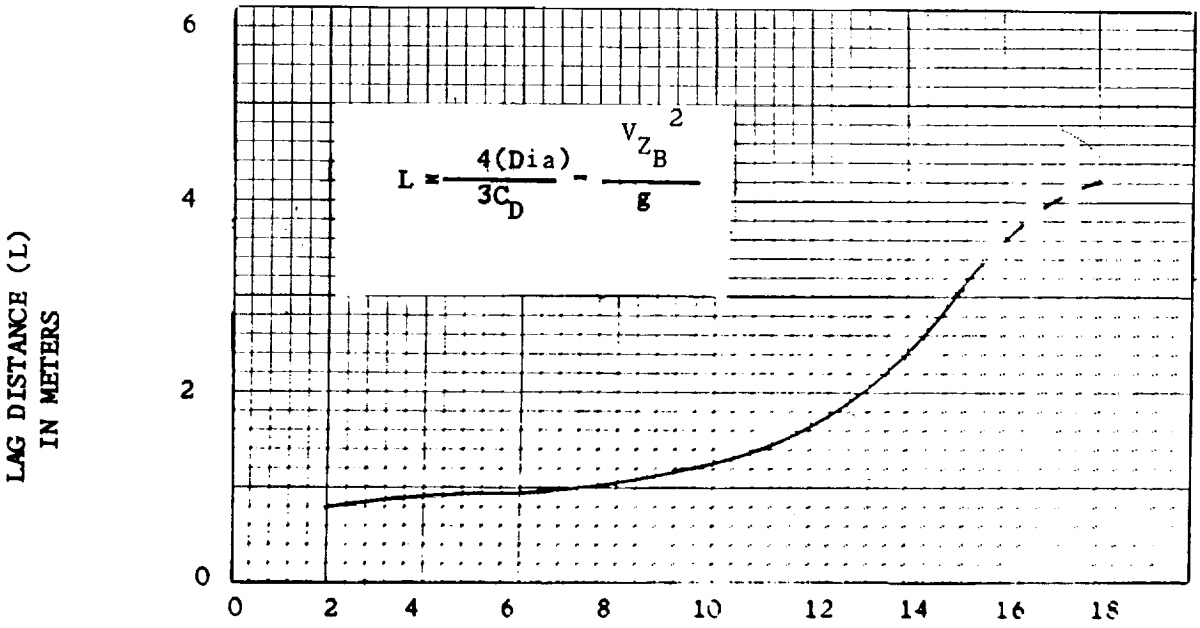

FIGURE 29 LAG DISTANCE (L) OF THE JIMSPHERE (BASED ON MASS RATIO) AS A FUNCTION OF ALTITUDE

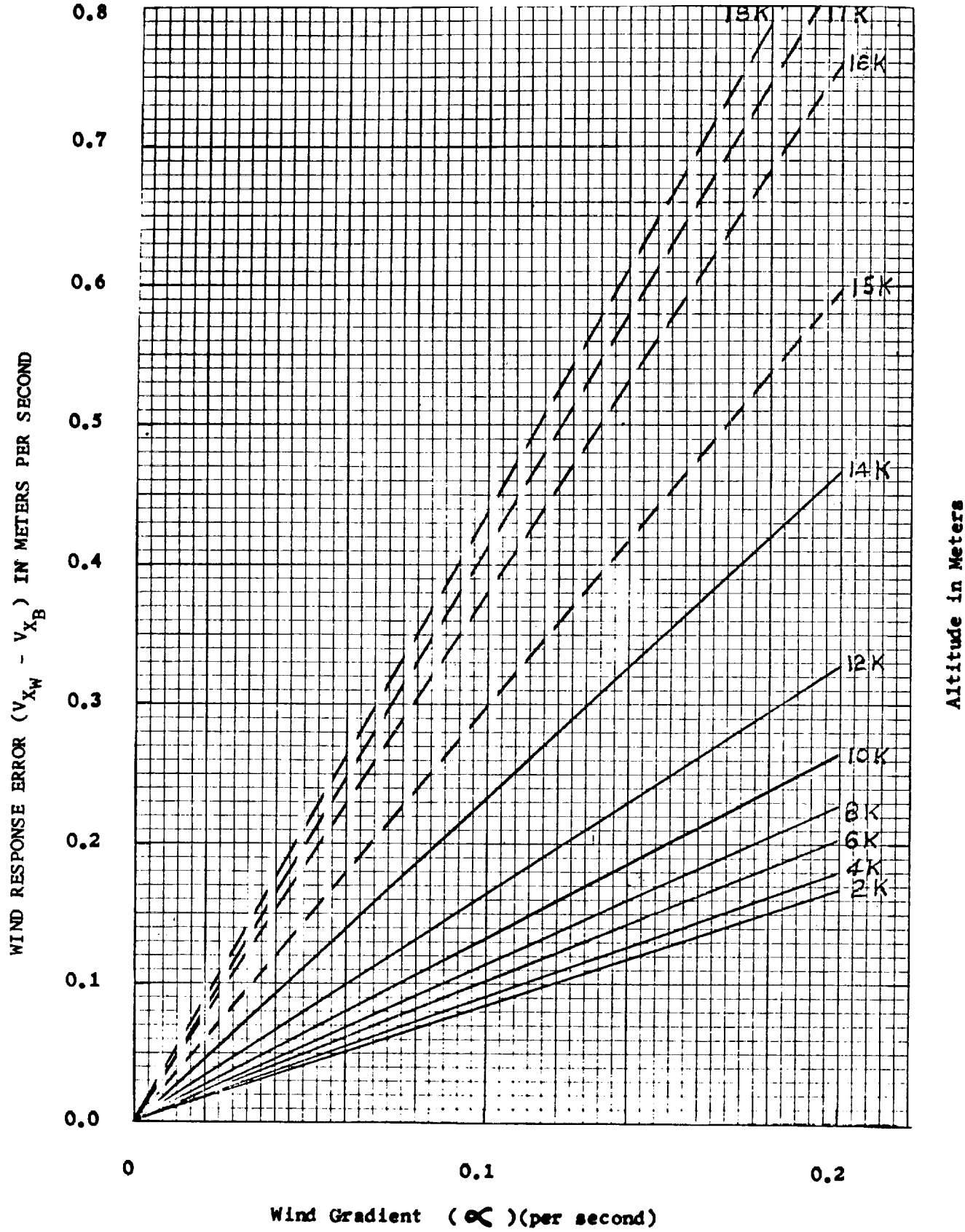

FIGURE 30 WIND RESPONSE ERROR (VELOCITY LAG) OF THE JIMSPHERE AS A FUNCTION OF WIND GRADIENT AT SEVERAL ALTITUDES

the Jimsphere is less than 0.2 meters per second for the highest wind gradient normally expected to be encountered (α = 0.1/sec). At 16,000 meters altitude this maximum expected wind response error increases to approximately 0.45 meters/second for a 0.1/sec wind gradient. It should be noted that the strong wind gradient conditions are generally encountered only when the actual wind velocities are quite high (10 meters per second or more).

The effects of Jimsphere velocity lag ($V_{X_W} - V_{X_B}$) on indicated wind gradients is presented in Section VIII.

C. Response Distance

The response distance (R) of a wind sensor is a characteristic coefficient of the sensor comparable to a system time constant except that it has the dimensions of length. When the wind sensor has traveled into the wind condition (step function or gradient) a distance $h-h_o$ = 3R it will have attained 95 percent of equilibrium conditions. The response distance (R) of the Jimsphere balloon is presented in Figure 31 as a function of altitude.

D. Distance Constant

The response capabilities of many different types of meteorological wind sensing instruments are analyzed by comparison of distant constants. For the Jimsphere the distant constant is defined as the horizontal distance the Jimsphere travels during the time it takes to acquire 63 percent of the wind velocity

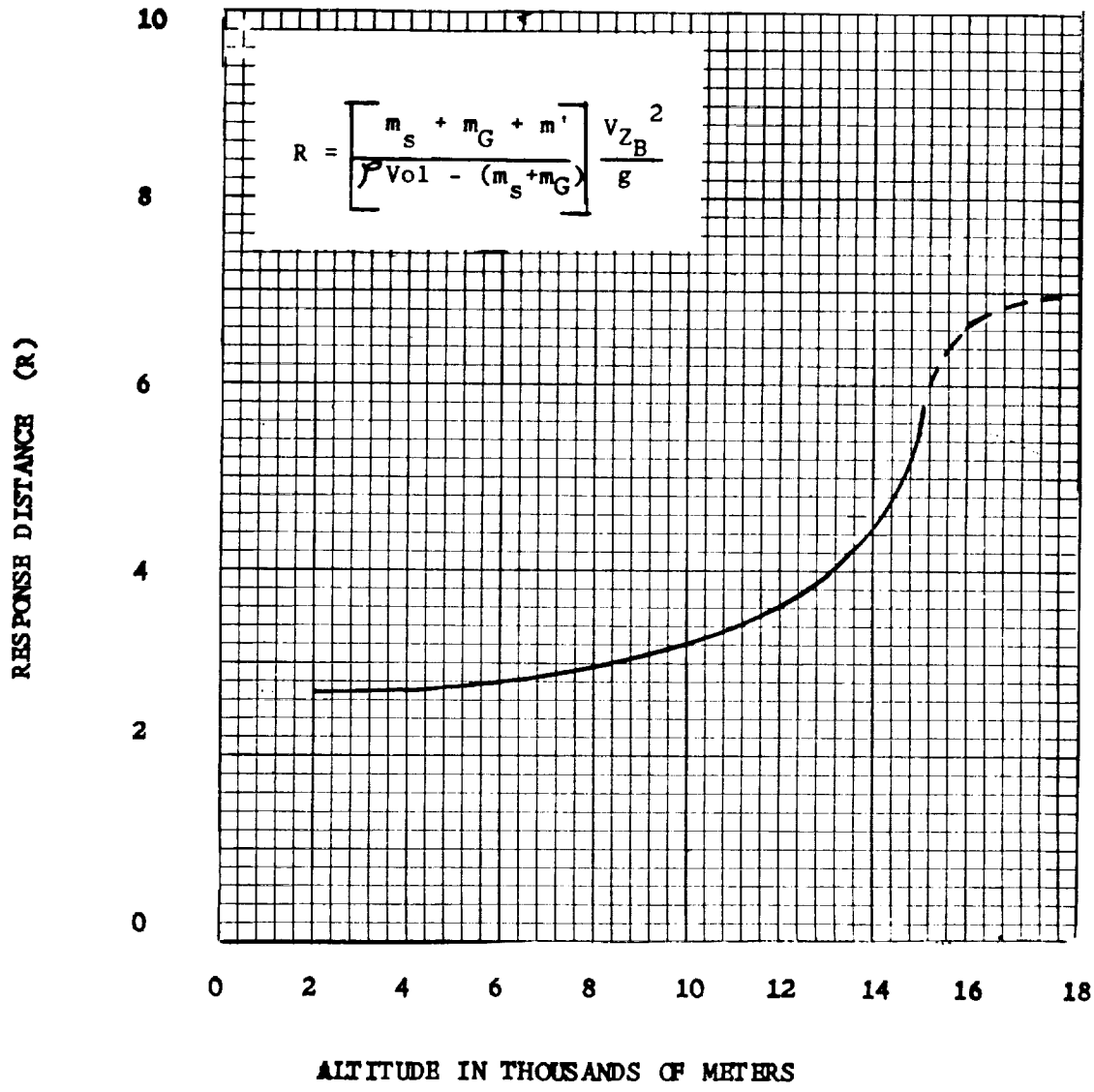

FIGURE 31 RESPONSE DISTANCE (R) OF THE JIMSPHERE AS A FUNCTION OF ALTITUDE

it is subjected to. The following assumptions are made:

1. The wind velocity is constant.
2. The Jimsphere is restrained and the air flow around the sphere established prior to release (the velocity of the Jimsphere is zero at time zero).
3. The Jimsphere is neutrally buoyant and therefore has no vertical velocity.

The equation of motion for the Jimsphere is then:

$$(m_s+m_G)\dot{V}_{X_B} = C_D\tfrac{1}{2}\rho S(V_{X_W} - V_{X_B})^2 + m'(\dot{V}_{X_W} - \dot{V}_{X_B}) \qquad (1)$$

For V_{X_W} = constant, $\dot{V}_{X_W} = 0$ and equation (1) becomes

$$(m_s+m_G+m')\dot{V}_{X_B} = C_D\tfrac{1}{2}\rho S(V_{X_W} - V_{X_B})^2 \qquad (2)$$

$$\text{Now } \dot{V}_{X_B} = \frac{dV_{X_B}}{dt} = \frac{dV_{X_B}}{dX}\,\frac{dX}{dt} = \frac{dV_{X_B}}{dX}\,V_{X_B} \qquad (3)$$

Substituting (3) into (2) and rearranging we have

$$\frac{V_{X_B}\,dV_{X_B}}{(V_{X_W}-V_{X_B})^2} = \frac{C_D\tfrac{1}{2}\rho S}{(m_s+m_G+m')}\,dX \qquad (4)$$

Integrating equation (4) from $V_{X_B} = 0$ to $V_{X_B} = 0.63\ V_{X_W}$, and from X = 0 to X and then evaluating for X at sea level conditions and $C_D = 0.75$, we find that

$$X = 1.83 \text{ meters.}$$

The Jimsphere distant constant as defined above is therefore 1.83 meters or 6 feet. This means that the Jimsphere will attain 63 percent of the wind velocity before traveling a distance equal to its diameter (2-meters).

VIII. JIMSPHERE WIND GRADIENT ERROR FACTORS

A. Definition

The Wind Gradient Error Factor (ξ_B) is defined as the ratio of the Wind Gradient to the velocity gradient of the balloon over the same altitude interval.

$$\text{Wind Gradient Error Factor } (\xi_B) = \frac{\text{Wind Velocity Gradient}}{\text{Balloon Velocity Gradient}}$$

The Wind Velocity Gradients and the Balloon Velocity Gradients are determined by the differences in the wind velocities and balloon velocities at the beginning and end of the altitude interval under consideration.

$$\text{Wind Gradient } (\alpha_W) = \frac{V_{X_{W_2}} - V_{X_{W_1}}}{h_2 - h_1} \qquad (1)$$

$$\text{Balloon Velocity Gradient } (\alpha_B) = \frac{V_{X_{B_2}} - V_{X_{B_1}}}{h_2 - h_1} \qquad (2)$$

B. Use of Wind Gradient Error Factors

Under presently used data reduction methods (Reference 3) the velocity gradient of the balloon as determined by radar track is considered essentially that of the wind. This is not exact because of the wind response error or velocity lag of the balloon to the wind.

To estimate what this error in indicated wind gradient might be, we have calculated Wind Gradient Error Factors for various

possible wind gradient conditions as illustrated in Figure 32. The assumption is made that the wind gradients are constant over the altitude intervals of interest.

For wind gradient conditions exemplified by Case I in Figure 32 the balloon velocity gradient in altitude interval h_1 to h_2 is of opposite direction but of smaller magnitude than the gradient of interval h_o to h_1. At the end of the altitude interval h_o to h_1 the Jimsphere velocity will be less than the wind velocity and at the end of the interval h_1 to h_2 the Jimsphere velocity is greater than the wind velocity. The result is that the velocity gradient of the balloon, as defined by equation (2), over interval h_1 to h_2 is much less than the actual wind gradient and the appropriate Wind Gradient Error Factor (ξ_B) must be applied to the observed balloon gradient to obtain the correct wind gradient. It should be noted here that the Wind Gradient Error Factor is one ($\xi_B = 1.0$) when there is no error in indicated wind as exemplified by Case 5 of Figure 32.

Observations of the wind profile data sheets from flight tests of the Jimsphere indicate that actual changes in wind gradients between altitude intervals is usually in the ranges exemplified by Cases 4 and 6 of Figure 32. In such instances the corrections needed are small and it is a very good assumption that the velocity gradient of the balloon is essentially that of the wind. If a wind profile indicates a large change in velocity over a short

Wind Velocity

----------Horizontal Velocity of Jimsphere

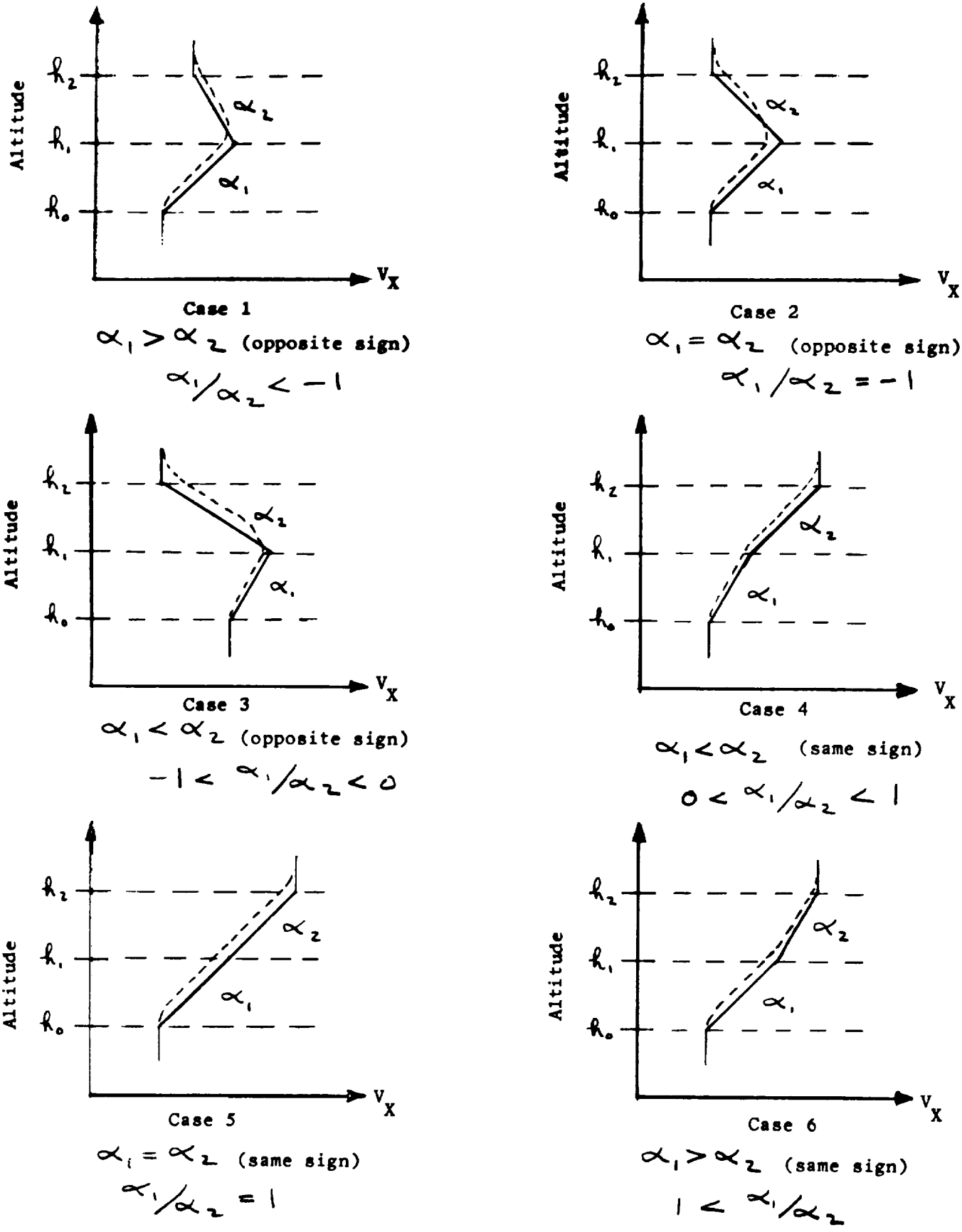

FIGURE 32 VARIOUS POSSIBLE WIND GRADIENT CONDITIONS

interval the Wind Gradient Error Factors presented here may be used to estimate how much greater the actual change in wind gradient may have been. It should be noted that velocities presented in wind profiles are averages over intervals (Reference 3) and for this reason are not necessarily indicative of constant wind gradients. The Wind Gradient Error Factors presented herein were established for constant wind gradients over the altitude intervals indicated. Figures 33 to 37 present Wind Gradient Error Factors for altitude intervals of 25, 50, 100, 200, and 300 meters.

It can be seen by examination of the above mentioned figures that the Wind Gradient Error Factors become quite insignificant for altitude intervals of 100 meters or more, especially at the altitudes less than 14,000 meters.

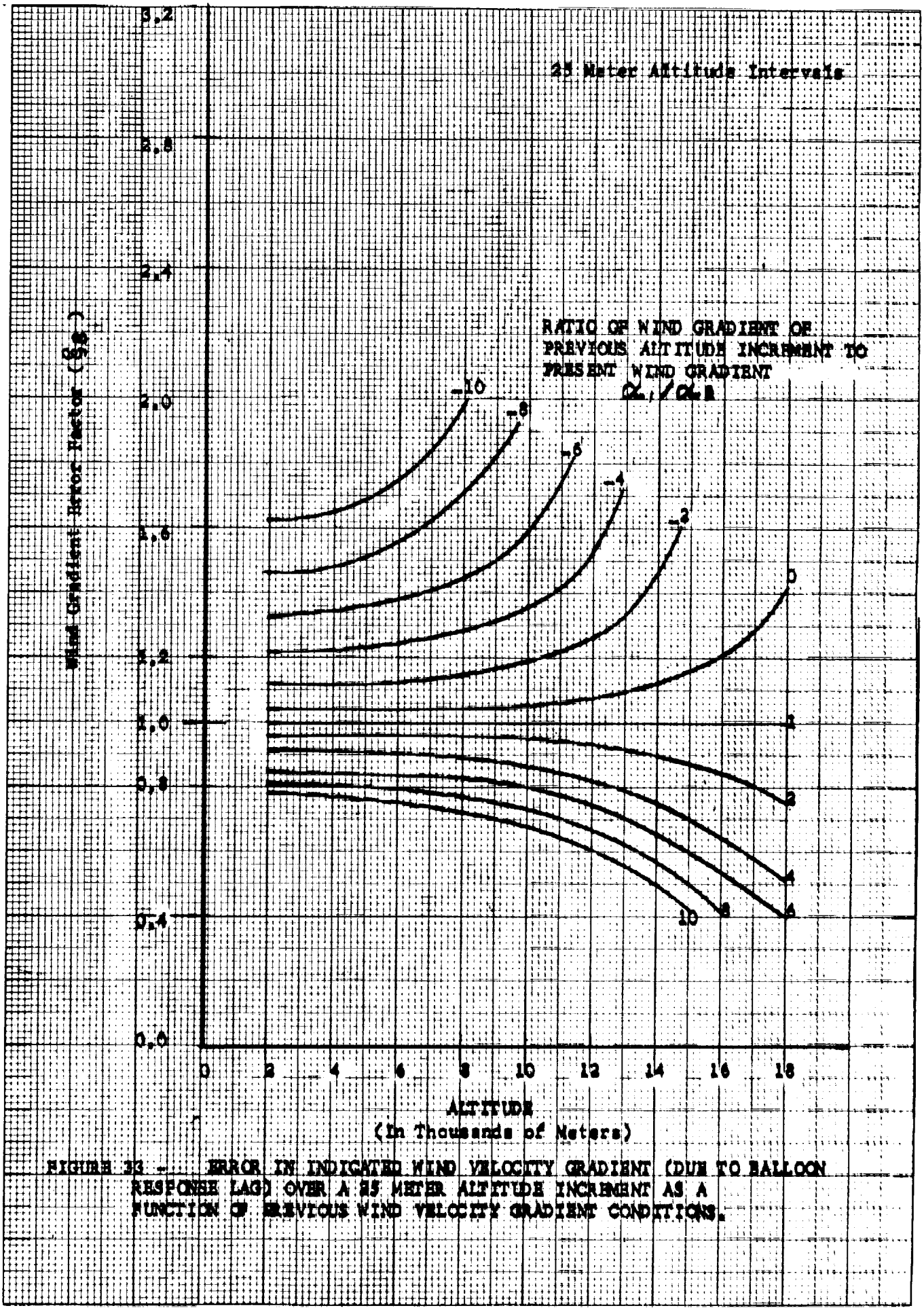

FIGURE 33 - ERROR IN INDICATED WIND VELOCITY GRADIENT (DUE TO BALLOON RESPONSE LAG) OVER A 25 METER ALTITUDE INCREMENT AS A FUNCTION OF PREVIOUS WIND VELOCITY GRADIENT CONDITIONS.

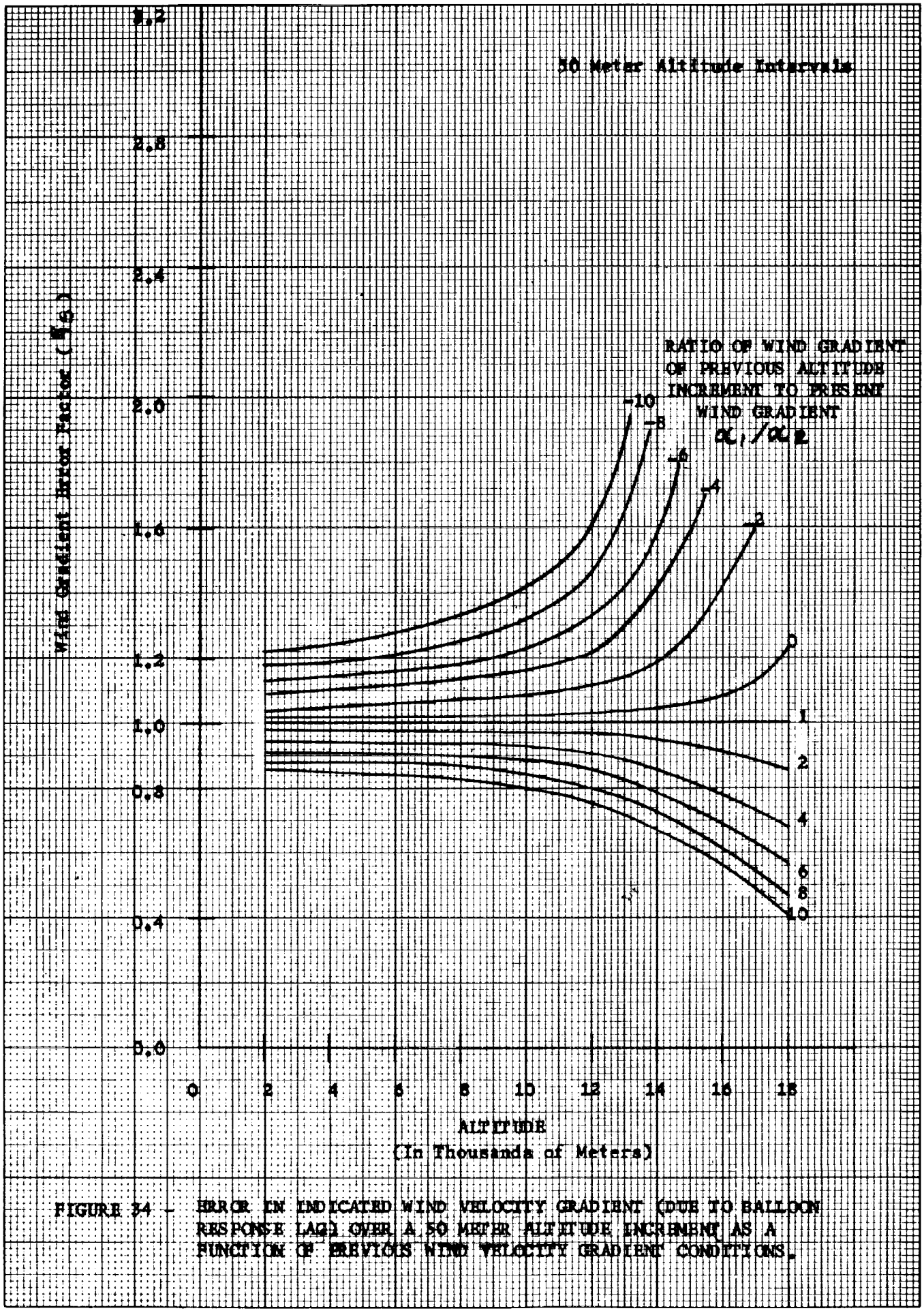

FIGURE 34 - ERROR IN INDICATED WIND VELOCITY GRADIENT (DUE TO BALLOON RESPONSE LAG) OVER A 50 METER ALTITUDE INCREMENT AS A FUNCTION OF PREVIOUS WIND VELOCITY GRADIENT CONDITIONS.

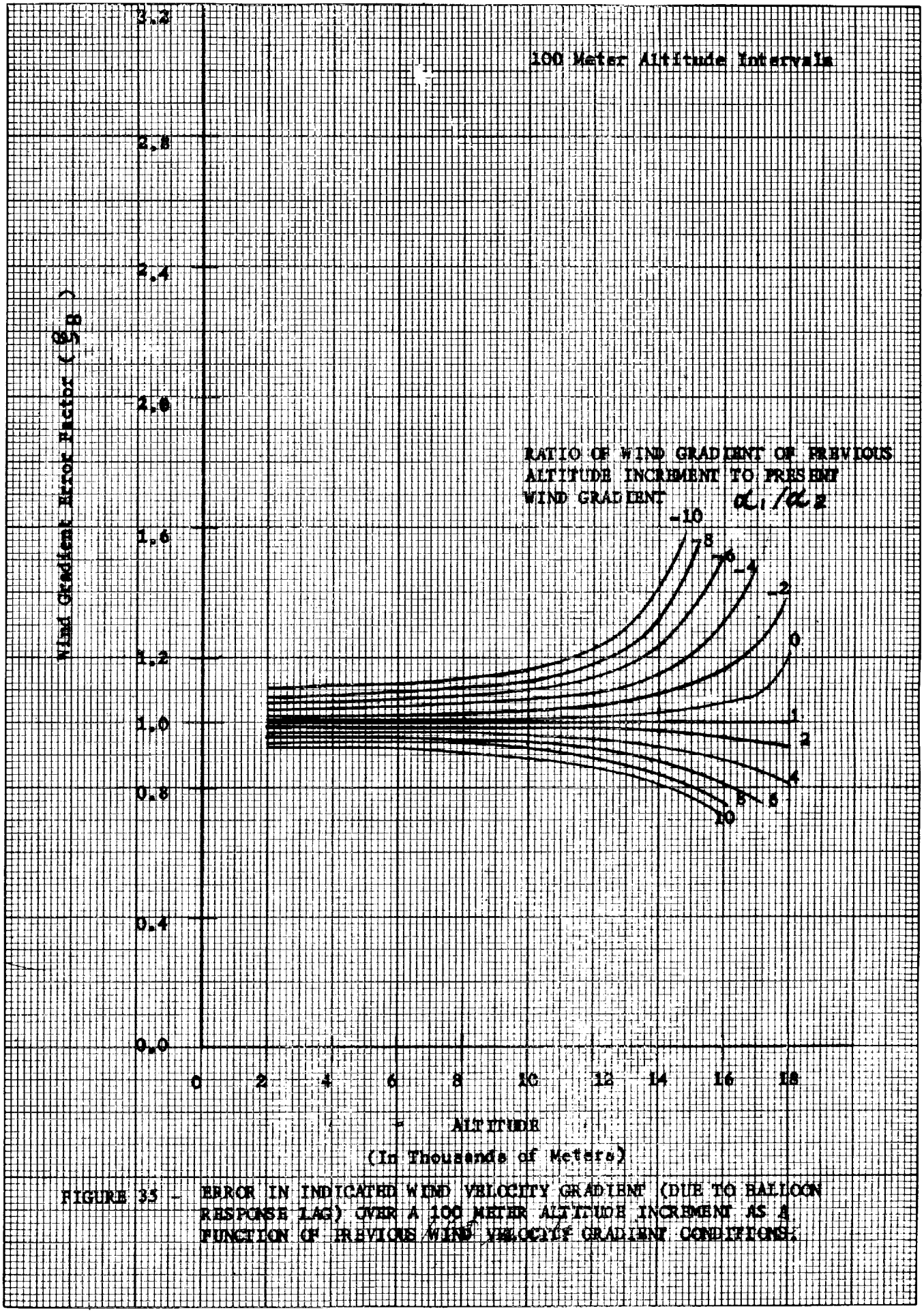

FIGURE 35 - ERROR IN INDICATED WIND VELOCITY GRADIENT (DUE TO BALLOON RESPONSE LAG) OVER A 100 METER ALTITUDE INCREMENT AS A FUNCTION OF PREVIOUS WIND VELOCITY GRADIENT CONDITIONS.

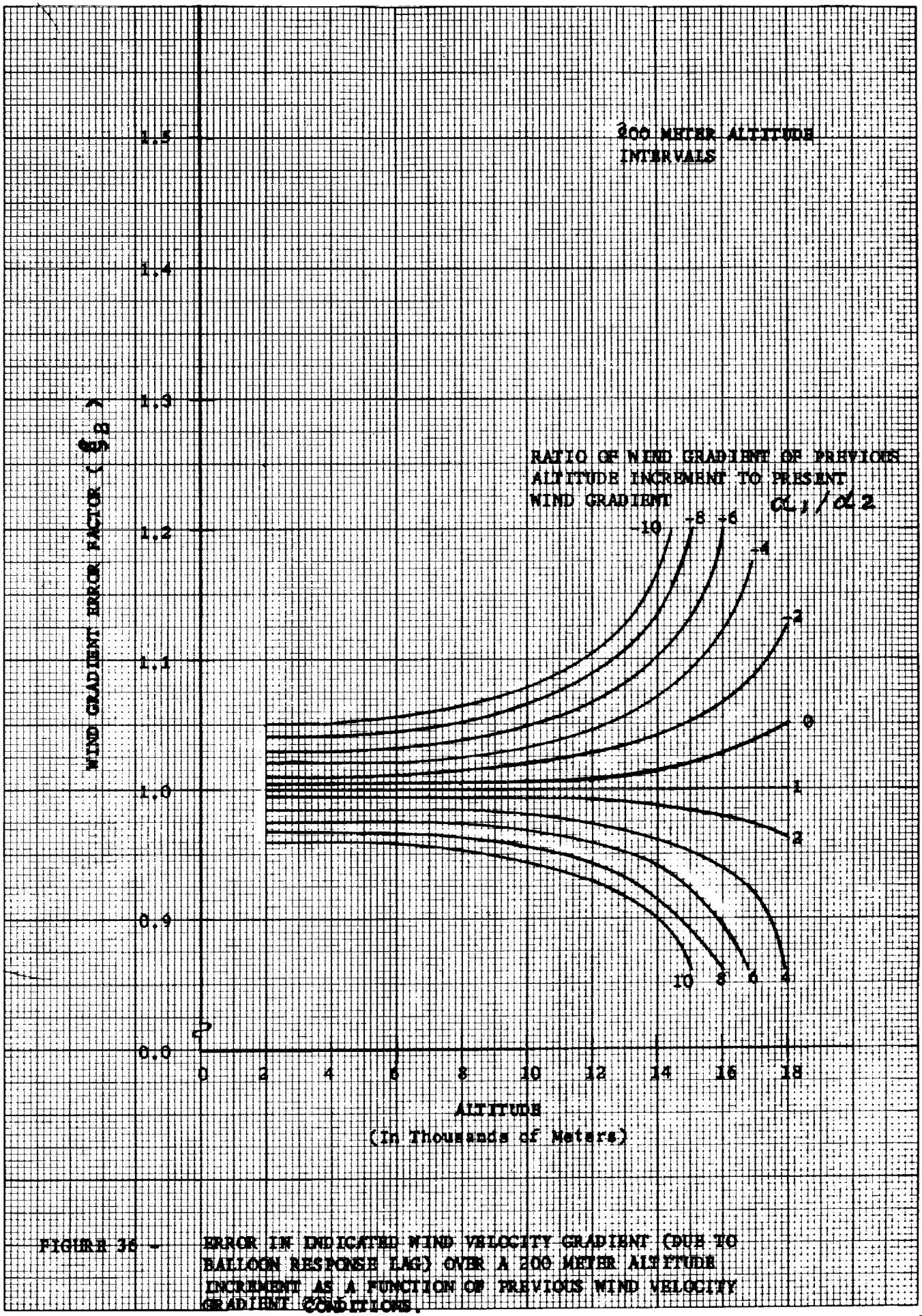

FIGURE 36 - ERROR IN INDICATED WIND VELOCITY GRADIENT (DUE TO BALLOON RESPONSE LAG) OVER A 200 METER ALTITUDE INCREMENT AS A FUNCTION OF PREVIOUS WIND VELOCITY GRADIENT CONDITIONS.

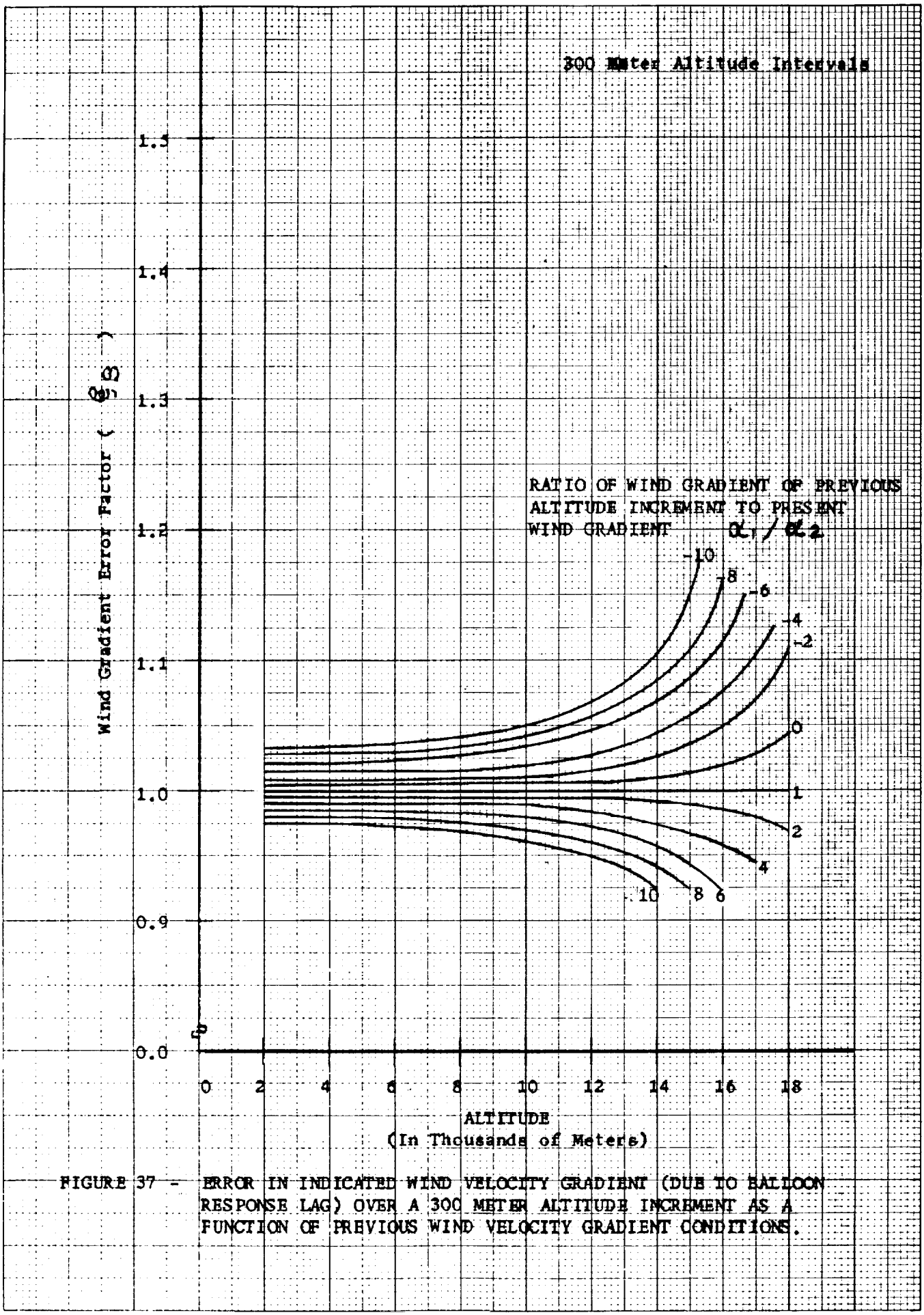

FIGURE 37 - ERROR IN INDICATED WIND VELOCITY GRADIENT (DUE TO BALLOON RESPONSE LAG) OVER A 300 METER ALTITUDE INCREMENT AS A FUNCTION OF PREVIOUS WIND VELOCITY GRADIENT CONDITIONS.

IX. SUMMARY AND CONCLUSIONS

The Engineering Development of Jimspheres having surface roughness elements molded into the surface of the sphere indicated that:

1. Roughness elements of truncated cone or full conical shape can be molded into the metalized Mylar material by conventional drape forming methods.
2. An increase in height or surface area of a roughness element requires additional spacing of the elements to allow forming into the Mylar material.

Jimspheres having 2-, 3-, and 4-inch high roughness elements molded into the surface were fabricated and flight tested. In addition, Jimspheres having 100 and 200 gram added weights were flight tested. These flight tests indicated that:

1. An increase in the number of roughness elements on the surface of the sphere increases the aerodynamic stability of the Jimsphere in flight.
2. An increase in the height of the roughness elements on the surface of the sphere increases the aerodynamic stability of the Jimsphere in flight.
3. Addition of a small mass at a point on the sphere decreases rotation and improves aerodynamic stability.

A joint analysis of these Jimsphere flight records by Schjeldahl personnel and Mr. James Scoggins of Marshall Space Flight Center indicated that a Jimsphere having the maximum possible number of three-inch high conical roughness elements and a 100 gram added weight (point

The Jimsphere Wind Sensor Balloon is a very sensitive, highly accurate system for attaining wind velocity and wind gradient measurements in the atmosphere between sea level and approximately 18,000 meters altitude.

mass) provided the greatest aerodynamic stability during flight. This Jimsphere designated as Model 3-7.5-398F was selected as the optimum configuration of those tested and subjected to further analysis and testing.

Wind tunnel tests of a model Jimsphere established a Drag Coefficient versus Reynolds number curve different than the classical drag curve of a smooth sphere. Analysis of Jimsphere flight data indicated that the drag coefficient of a full size Jimsphere in flight, at supercritical R_e, is nearly double that of a model subjected to wind tunnel testing.

Apparent mass tests determined that the apparent mass factor for a Jimsphere is only slightly different than the theoretical value of apparent mass for a smooth sphere.

Theoretical analysis of the Jimsphere reveal that:

1. The lag distance of the Jimsphere velocity profile to the wind profile is independent of apparent mass effects.
2. The lag distance of the Jimsphere is less than one meter below 6000 meters altitude and less than two meters (one balloon diameter) below 13,000 meters altitude.
3. The Jimsphere distant constant at sea level conditions is less than one balloon diameter.
4. Velocity gradients as determined from track of the Jimsphere Wind Sensor are nearly identical to wind gradients except for conditions of large reversals in wind gradient.

LIST OF REFERENCES

1. Scoggins, James R., "Aerodynamics of Spherical Balloon Wind Sensors". Journal of Geophysical Research, Volume 69, pp. 591 - 598, 1964.

2. Scoggins, James R., "Spherical Balloon Wind Sensor Behavior". Paper presented at the American Meteorological Society Meeting, Atlantic City, New Jersey, March 1964. Journal of Applied Meteorology, January 1965.

3. Scoggins, James R., "An Evaluation of Detail Wind Data as Measured by the FPS-16 Radar/Spherical Balloon Technique". Report MPT-AERO-62-38, NASA Marshall Space Flight Center, Huntsville, Alabama, April 20, 1962.

4. Atlantic Missile Range Reference Atmosphere for Cape Kennedy, Florida, (Part 1), Inter-Range Instrumentation Group of the Range Commanders Council, IRIG Document 104-63, September 1963.

5. Eckstrom, C. V., "Research and Development of Rigid, Rising, Radar Reflective Balloons", Volume II, Balloon Design, Final Report on Contract AF 19 (628)-2993, July 1963.

6. MacCready, Jr., Paul B. and Henry R. Jex, "Study of Sphere Motion and Balloon Wind Sensors", NASA TMX-53089, July 27, 1964.

7. Research and Development of Rigid Rising Radar Reflective Balloons, Volume I "The Wind Response Error of an Ascending Balloon Under Consideration of Apparent Mass", G. T. Schjeldahl Company, Northfield, Minnesota, Final Report on Contract AF 19(628)-2393.

8. Johnston, K. D., Response of Spherical Balloons to Wind Gusts, Memorandum M-AERO-A-12-62, NASA Marshall Space Flight Center, Huntsville, Alabama, March 5, 1962.

9. Reed III, Wilmer H., "Dynamic Response of Rising and Falling Wind Sensors with Applications to Estimates of Wind Loads on Launch Vehicles", NASA TN D-1821, October 1963.

10. Pope, Allen, "Wind Tunnel Testing", John Wylie and Sons, Inc., New York, New York, 1954.

APPENDIX A

Vertical rate of rise data from flights 8962, 8920, 8940, 8959, 8960, 8964, 8966, 8967, 8968m 8970 of Jimspheres Model 3-7.5-398F during December 1964.

VERTICAL RISE RATE OF JIMSPHERE BALLOON JIMSPHERE BALLOON TEST - DEC. 1964 CAPE KENNEDY, FLORIDA

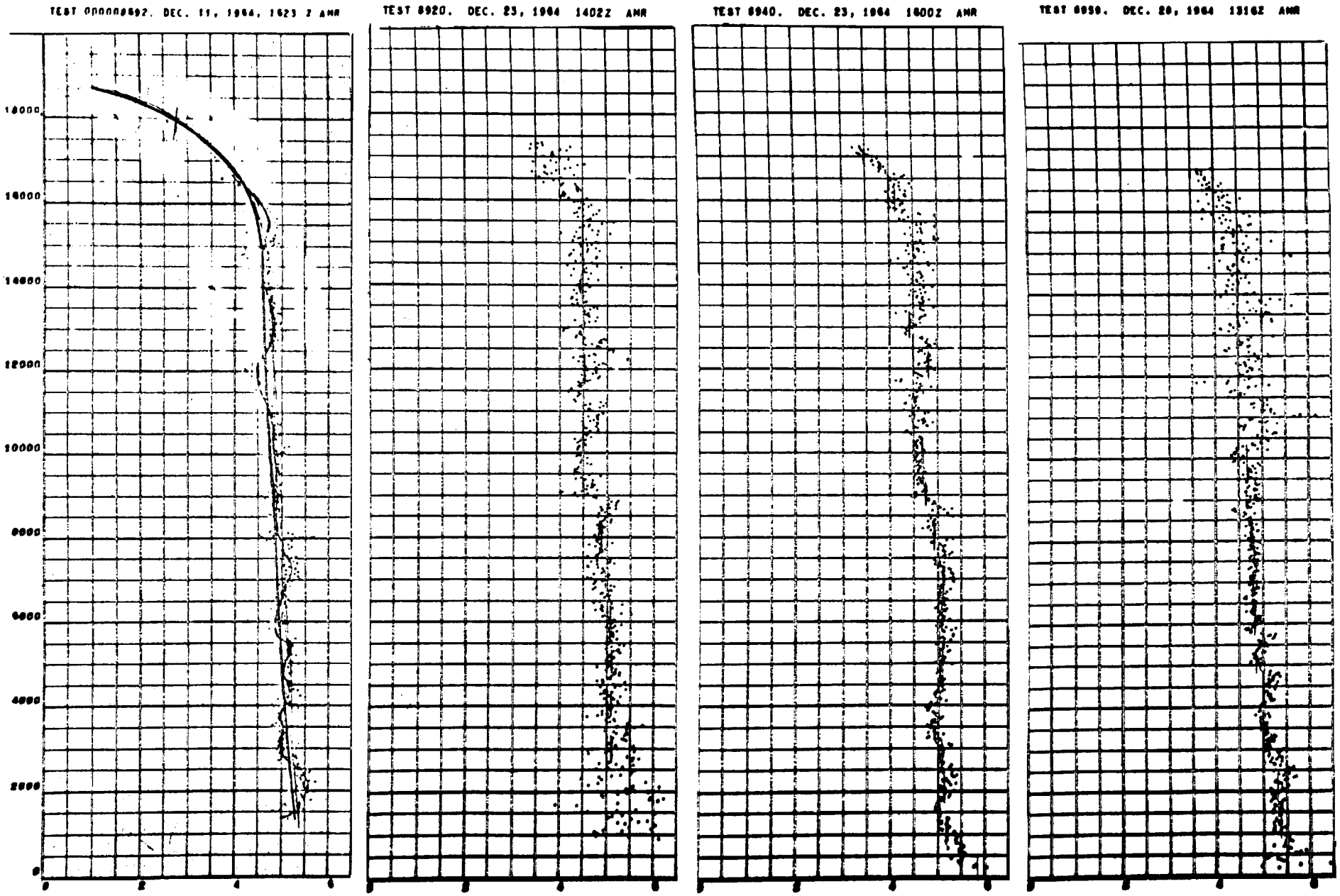

VERTICAL RISE RATE OF JIMSPHERE BALLOON JIMSPHERE BALLOON TEST - DEC. 1964 CAPE KENNEDY, FLORIDA

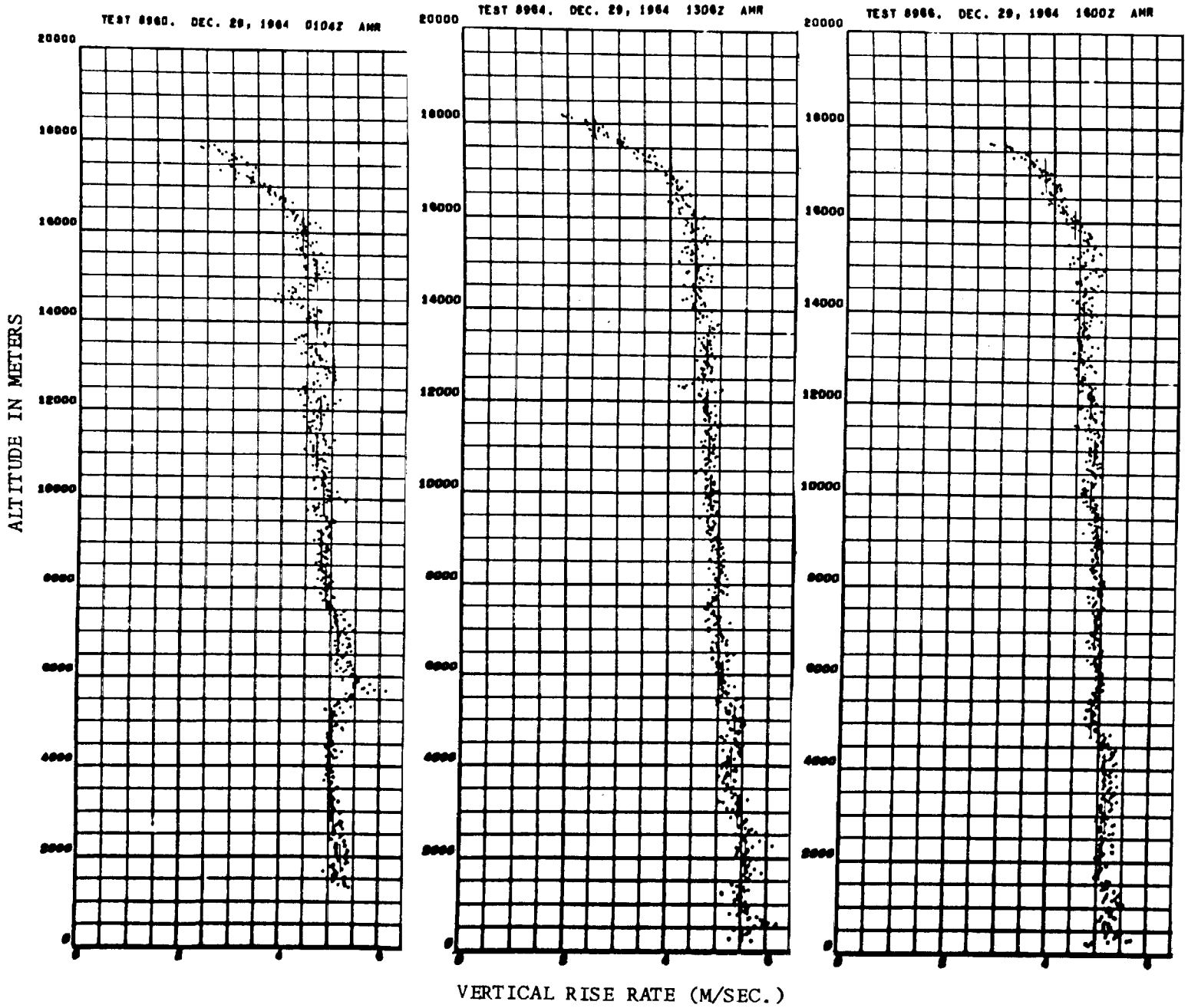

VERTICAL RISE RATE OF JIMSPHERE BALLOON JIMSPHERE BALLOON TEST - DEC. 1964 CAPE KENNEDY, FLORIDA

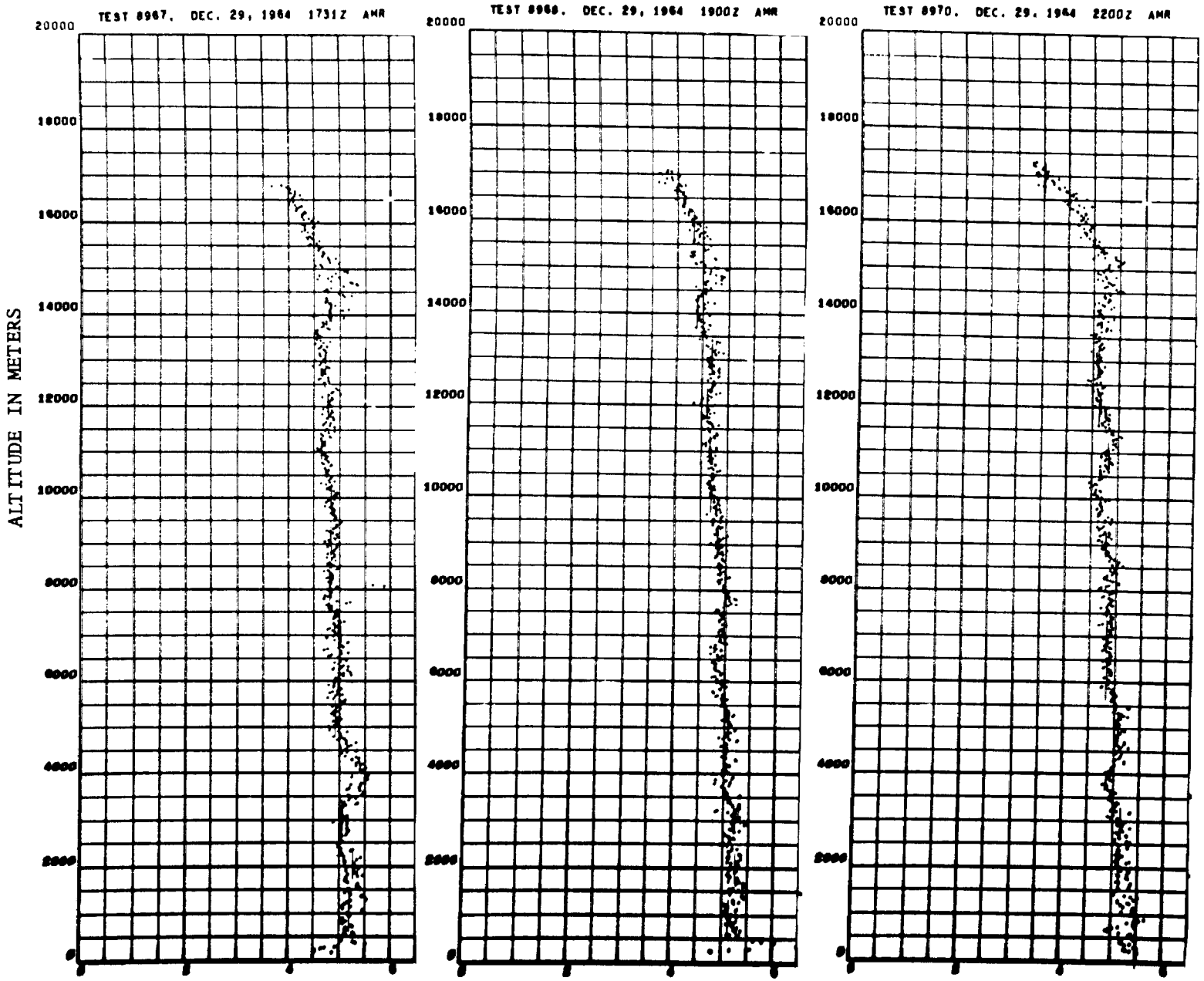

APPENDIX B

DERIVATION OF THE EQUATION FOR JIMSPHERE WIND RESPONSE ERROR

The Wind Response Error is defined as the difference in horizontal velocity between the wind and the balloon ($V_{X_W} - V_{X_B}$). The magnitude of the wind response error can be determined from a solution of the equations of motion for the balloon. These equations of motion are:

X (horixontal)

$$(m_s+m_G)\dot{V}_{X_B} = C_D\tfrac{1}{2}\rho S V_R(V_{X_W} - V_{X_B}) + m'(\dot{V}_{X_W} - \dot{V}_{X_B}) \qquad (1)$$

Z (vertical)

$$(m_s+m_G)\dot{V}_{Z_B} = -C_D\tfrac{1}{2}\rho V_R V_{Z_B} S - (m_s+m_G)g + \rho g\ VOL \qquad (2)$$

The following assumptions are necessary:

1. The wind gradient is constant over the altitude interval under consideration.
2. The wind gradient is not of such magnitude to cause a change in the balloon ascent rate (α = 0.28 per second or less). (Reference 8)

Assuming that the vertical rise rate (V_{Z_B}) does not change (as stated in assumption 2), then $\dot{V}_{Z_B} = 0$ and equation (2) simplifies to:

$$V_R = \frac{\rho g\ VOL - (m_s+m_G)g}{C_D\tfrac{1}{2}\rho Z V_{Z_B}} \qquad (3)$$

Substituting equation (3) into equation (1) we now have:

$$(m_s+m_G)\dot{V}_{X_B} - m' \frac{d}{dt}(V_{X_W} - V_{X_B}) = \frac{(V_{X_W} - V_{X_B})}{V_{Z_B}} \left[\rho g \text{ VOL} - (m_s+m_G)g\right] \quad (4)$$

For constant wind gradients (assumption 1)

$$\dot{V}_{X_W} = \frac{dV_{X_W}}{dh}\frac{dh}{dt} = \alpha V_{Z_B} \quad (5)$$

$$\text{and } V_{X_W} = V_{X_{W_o}} + \alpha(h-h_o) \quad (6)$$

in addition

$$\dot{V}_{X_B} = \frac{dV_{X_B}}{dh}\frac{dh}{dt} = \frac{dV_{X_B}}{dh} V_{Z_B} \quad (7)$$

Substituting equations (5), (6) and (7) into equation (4) and rearranging we have a differential equation of the form

$$\frac{dV_{X_B}}{dh} + PV_{X_B} = Q + Zh \quad (8)$$

$$\text{where } P = \left[\frac{\rho \text{VOL} - (m_s+m_G)}{m_s+m_G+m'}\right] \frac{g}{V_{Z_B}} \quad (9)$$

$$Q = \frac{m'\alpha}{m_s+m_G+m'} + P(V_{X_{W_o}} - \alpha h_o) \quad (10)$$

$$Z = \alpha P \quad (11)$$

Setting the right hand side of equation (8) equal to zero results in the homogeneous equation

$$\frac{dV_{X_B}}{dh} + PV_{X_B} = 0 \quad (12)$$

$$\frac{dV_{X_B}}{V_{X_B}} = -P\, dh \quad (13)$$

$$V_{X_B} = K_1 e^{-P(h-h_o)} \tag{14}$$

A solution for the inhomogeneous equation (8) is:

$$V_{X_B} = K_2(h-h_o) + K_3 = K_2h - K_2h_o + K_3 \tag{15}$$

$$\frac{dV_{X_B}}{dh} = K_2 \tag{16}$$

$$K_2 + P\left[K_2(h-h_o) + K_3\right] = Q + Zh \tag{17}$$

$$(1)\ PK_2 = Z \text{ and } K_2 = Z/P \tag{18}$$

$$(2)\ K_2 - PK_2h_o + PK_3 = Q \text{ and } K_3 = \frac{Q - Z/P + Zh_o}{P} \tag{19}$$

$$V_{X_B} = \frac{Z}{P}(h) + \frac{Q - Z/P}{P} \tag{20}$$

Adding the homogeneous and inhomogeneous equations (14) and (20) gives

$$V_{X_B} = K_1 e^{-P(h-h_o)} + \frac{Z}{P}(h) + \frac{Q - Z/P}{P} \tag{21}$$

For the general case where $V_{X_B} = 0$ when $h = h_o$

$$K_1 = V_{X_{B_o}} - \frac{Z}{P} h_o - \frac{Q - Z/P}{P} \tag{22}$$

and equation (21) is now

$$V_{X_W} - V_{X_B} = (V_{X_W} - V_{X_B})_o\, e^{-\frac{(h-h_o)}{R}} + \alpha L\left[1 - e^{-\frac{(h-h_o)}{R}}\right] \tag{23}$$

$$\text{Where } L = \left[\frac{m_s+m_G}{\rho VOL-(m_s+m_G)}\right] \frac{V_{Z_B}^{\,2}}{g} \tag{24}$$

$$\text{and } R = \left[\frac{m_s+m_G+m'}{\rho VOL - (m_s+m_G)}\right] \frac{V_{Z_B}^{\,2}}{g} \tag{25}$$

APPENDIX C

STUDY OF MODIFIED SPHERES

A study of Jimsphere flight test movies by NASA/MSFC personnel resulted in the observation that horizontal displacements of the balloon were usually accompanied by a rotation of the sphere. The observations indicated the sphere rolled in the direction of horizontal movement. In an effort to increase the stability of the Jimsphere and prevent rotation, ballast weights were added to the load patch of the sphere. Ballasting did reduce sphere rotational and horizontal movements, however some sphere rotation still existed. Ballast weights of 100 to 200 grams were testd. A ballast weight of 100 grams appeared to provide the best overall performance and was standardized. The basic weight of the Jimsphere without ballast is approximately 300 grams.

In an effort to learn more about sphere induced motion problems and sphere rotation, a series of experimental spheres were fabricated and flight tested. Movie records were made of the flights and standard Jimspheres were flown with the experimental spheres for reference purposes.

The first type experimental sphere fabricated is shown in Figure 38. It was anticipated that the Jimsphere gores would generate more drag than the smooth gores and the sphere would travel through the air with the smooth hemisphere up. All valves, the load patch, and the ballast weight are located at the intended bottom of the sphere. Visual observation of the flight indicated that the sphere would rotate about a horizontal axis as much as 60 degrees and review of the motion pictures

confirmed this.

A second type experimental sphere, as shown in Figures 39 and 40, was then fabricated. This sphere has six very large projections, located one each on every other gore. The point of the projection is located midway between the equator of the sphere and the lower end cap. This configuration did eliminate roll about the axis of flight, but did not eliminate rotation about the horizontal axis.

The third experimental sphere fabricated, incorporated regular Jimsphere gores and six large projections of the type shown in Figure 41. A photo of the fabricated sphere is shown in Figure 42. It was hoped that air flow off the tips of the larger projections would stabilize the air flow in the wake of the sphere.

A fourth experimental sphere, shown in Figure 43, was also fabricated. The purpose of the tubular extensions on the aft surface is to allow air flow to become attached to these secondary structures and then form individual wakes. This experimental, modified Jimsphere seemed stable in flight. However, because the tubular structures were also inflated with helium, the unit was not correctly balanced and had a tendency to float about 45 degrees to 90 degrees from vertical and in one case even inverted in flight.

None of the modified Jimspheres performed as well as the standard Jimspheres previously tested and in some instances considerable spiral motion was noticeable for the modified Jimspheres.

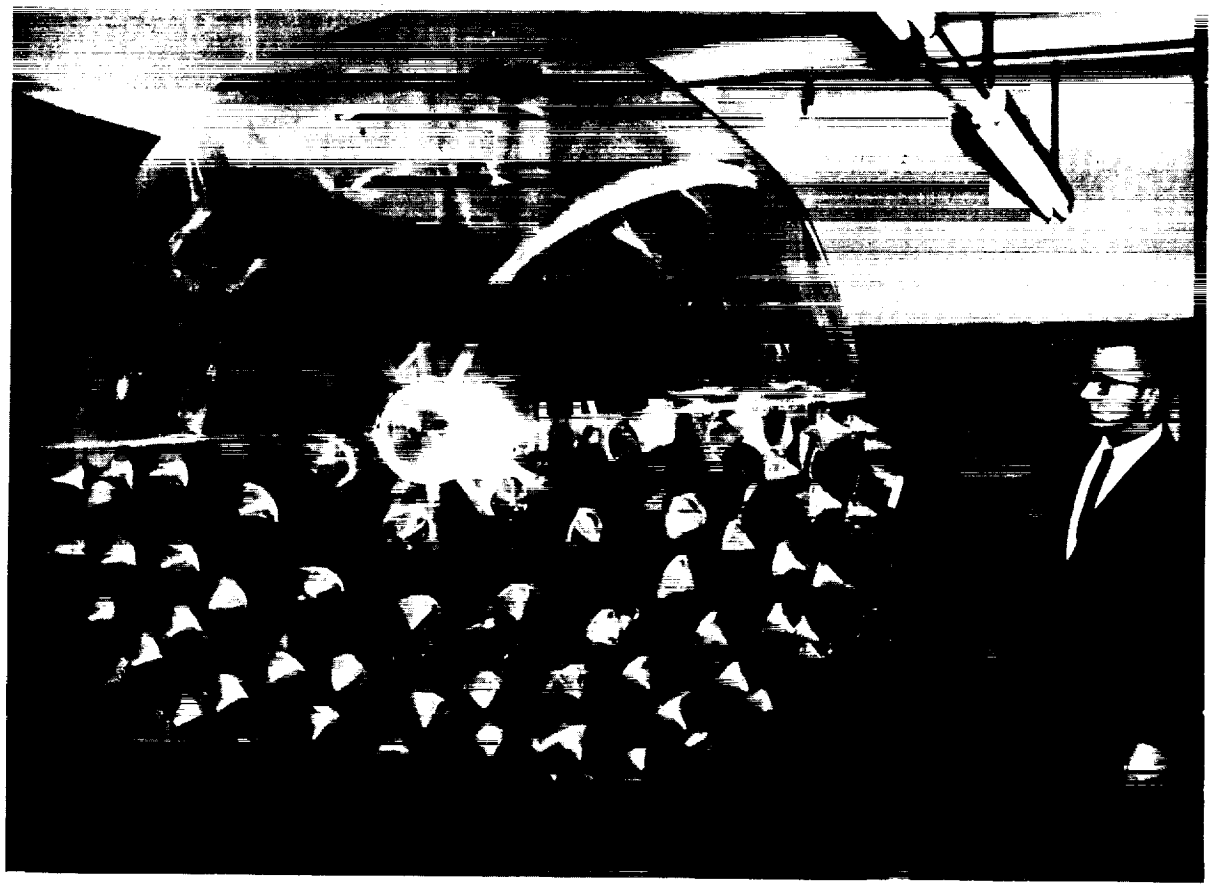

Figure 38. Experimental Sphere with Half Smooth Gores and Half Jimsphere Gores.

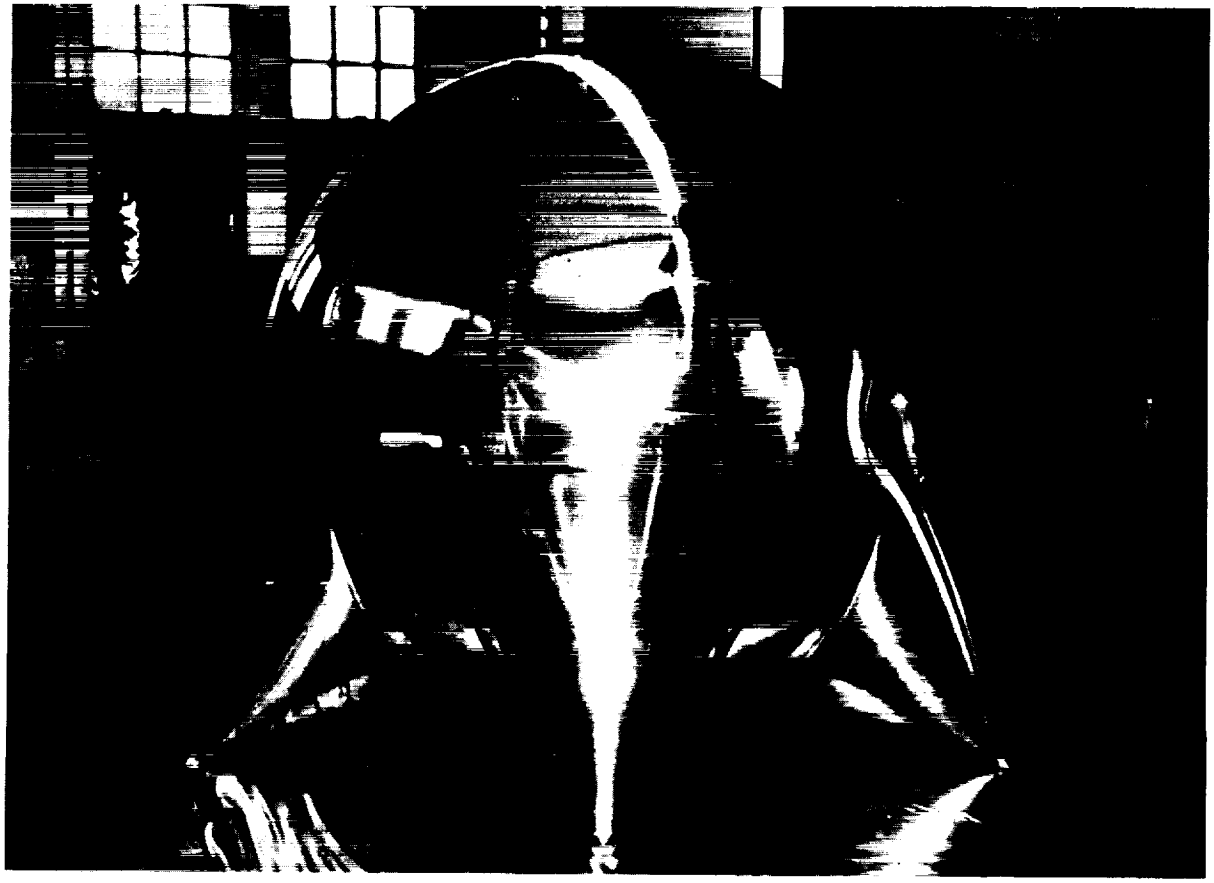

Figure 39. Side View of Experimental Smooth Sphere with Six Extra Large Projections.

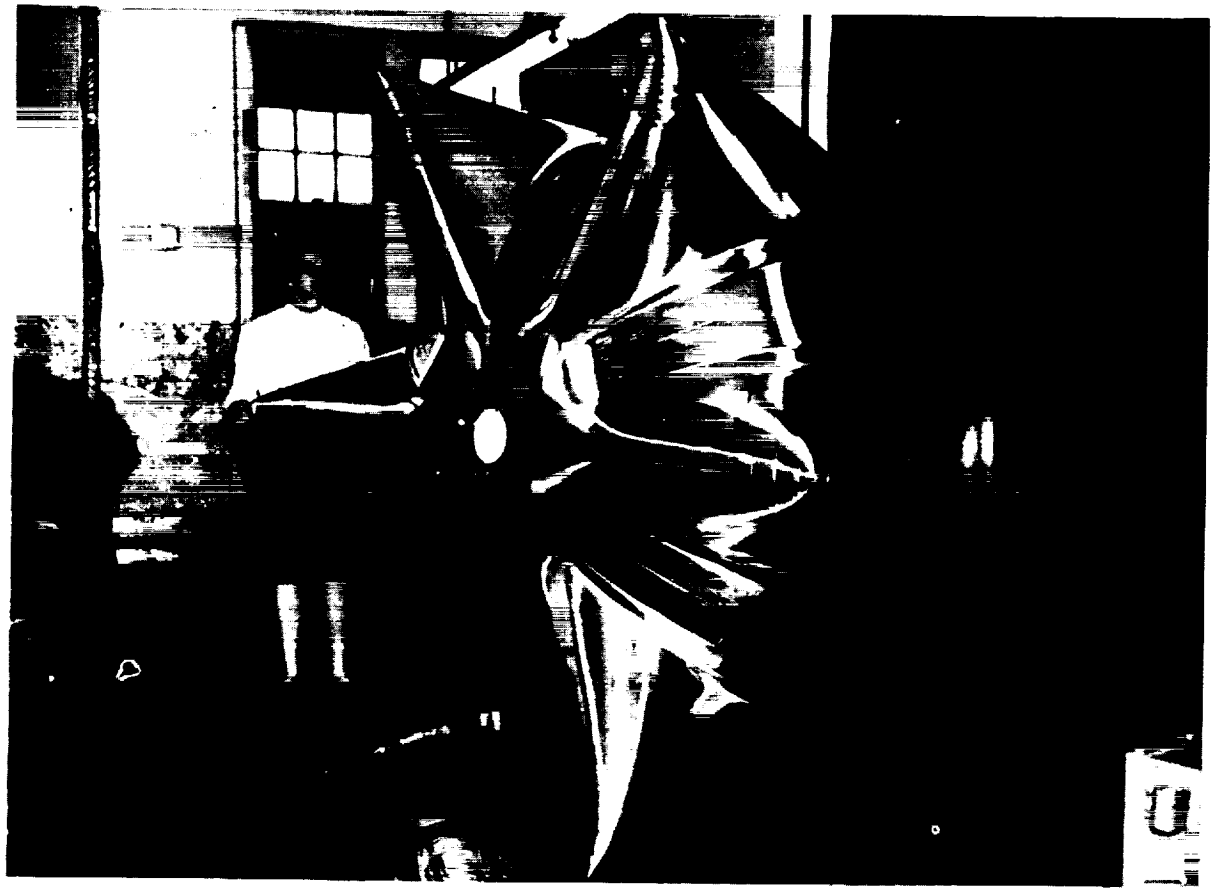

Figure 40. Bottom View of Experimental Smooth Sphere with Six Extra Large Projections.

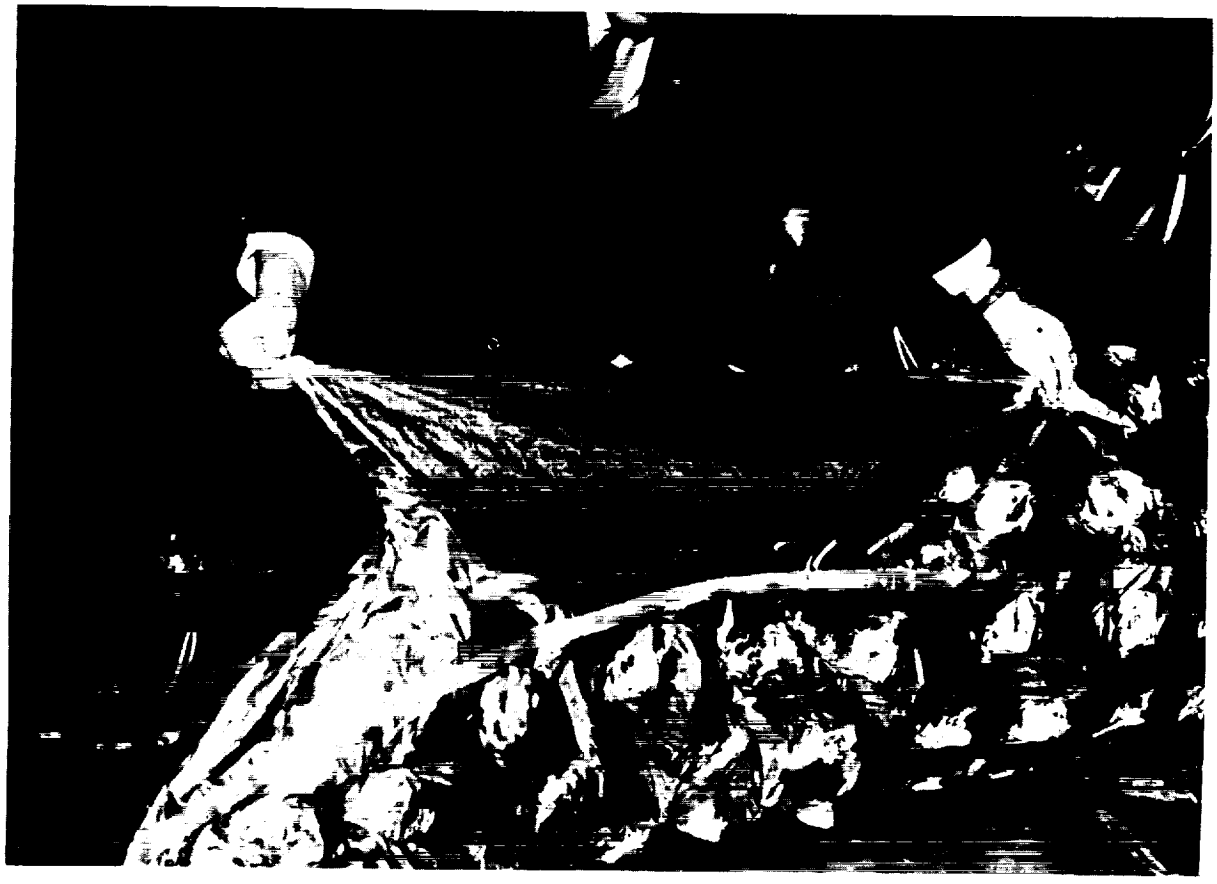

Figure 41. View of Uninflated Large Projection on a Modified Jinsphere.

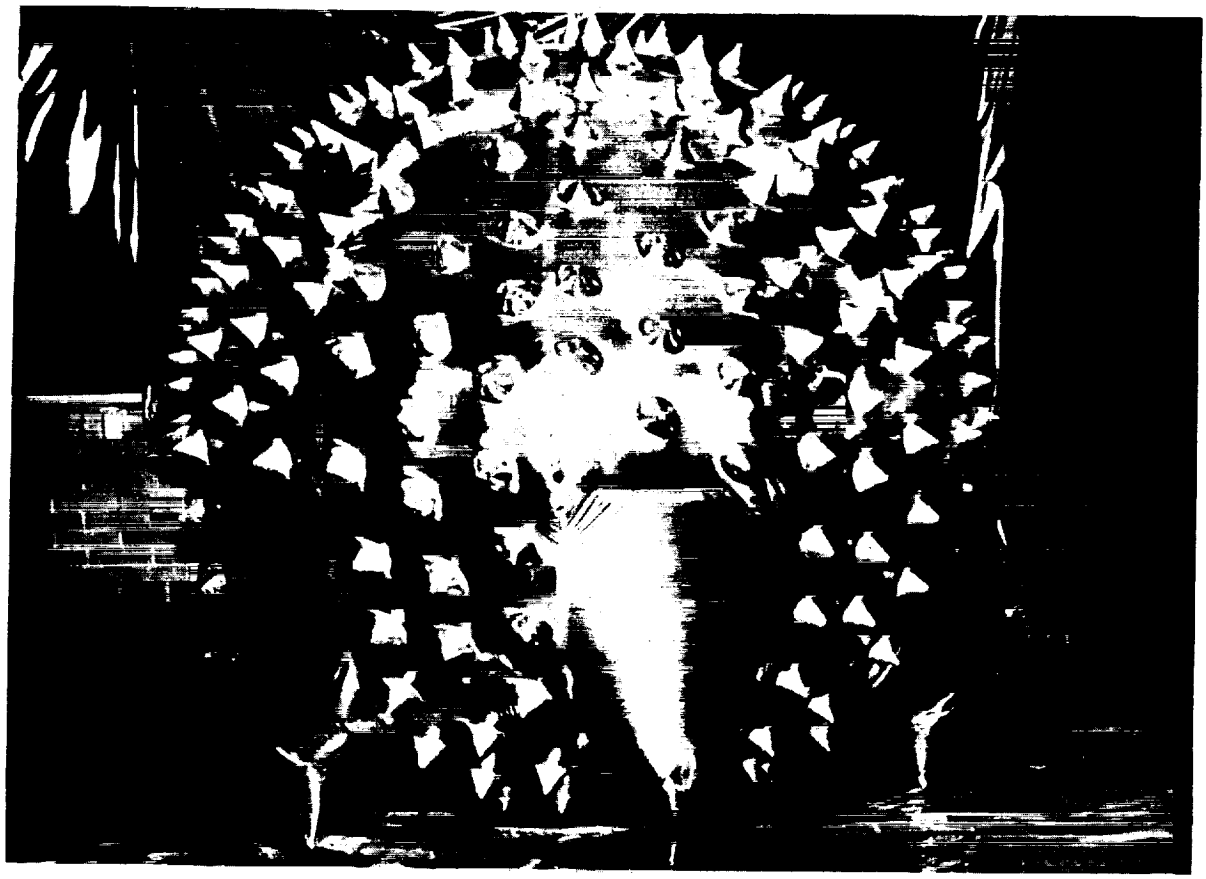

Figure 42. Modified Jimsphere with Six Large Conical Projections Pointing Aft.

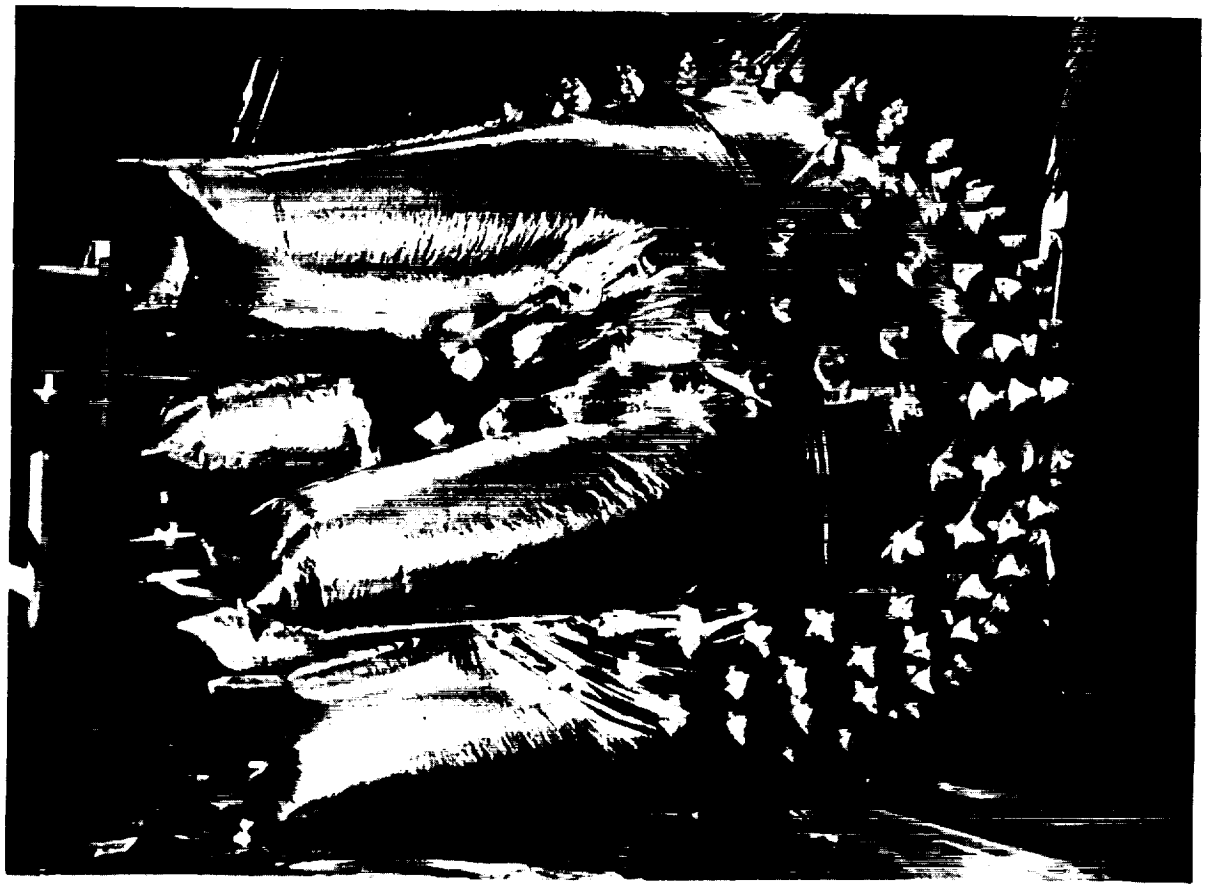

Figure 43. Modified Jimsphere with Six Tubular Extensions Projecting Aft